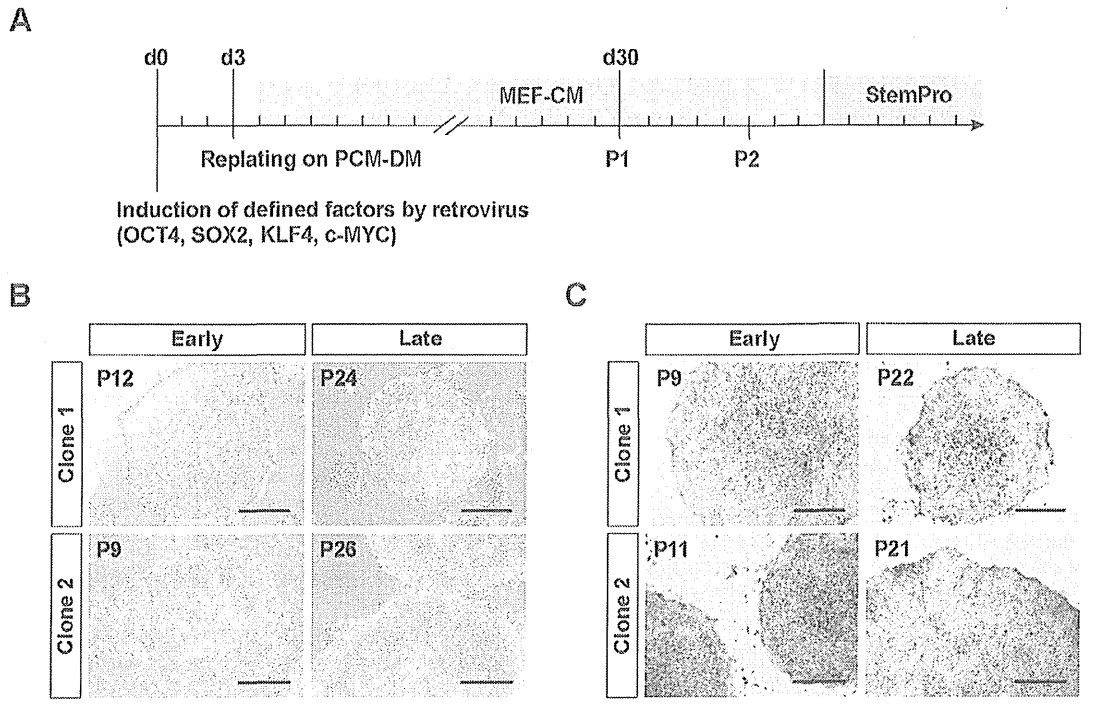

Figure 1. Generation of hiPSCs on PCM-DM. A) Schematic diagram for generating hiPSCs on PCM-DM. B) Representative morphology of the hiPSCs on PCM-DM at early and late passages. C) Alkaline phosphatase (ALP) staining of hiPSCs generated on PCM-DM. P, passage number. Scale bar = 500 μm.
doi:10.1371/journal.pone.0055226.g001

anti-SSEA-4 (MC-813-70, Chemicon International Inc., Temecula, CA), anti-SSEA-3 (MC-631, Chemicon), anti-TRA-1-60 (TRA-1-60, Chemicon), anti-TRA-1-81 (TRA-1-81, Chemicon). After being washed, the cells were incubated with the appropriate secondary antibodies (Alexa-488-conjugated anti-mouse IgG, anti-mouse IgM, or anti-rat IgM, Molecular Probes, Eugene, OR) for 30 min at 4°C. The stained samples were analyzed by FACS Calibur flow cytometer (BD Biosciences, San Jose, CA).

Microarray Analysis

Total RNA (100 ng) was used to synthesize aRNA using the 3′ IVT Express Kit, according to the manufacturer's instructions (Affymetrix Inc., Santa Clara, CA). After aRNA purification, 15 μg of aRNA was fragmented and hybridized with a pre-equilibrated GeneChip array (Human Genome U133 Plus 2.0 gene expression array, Affymetrix) at 45°C for 16 hours. The GeneChip array was then washed, stained, and scanned according to the manufacturer's instructions. The gene expression data were extracted using Affymetrix Expression Console software, and the Pearson's coefficient of correlation was calculated for each pair of samples. Hierarchical cluster analysis was carried out using the "Manhattan" method for the similarity measurement and the "complete" method for linkage. These analyses were performed using GeneSpring GX software (Agilent Technologies, Inc., Santa Clara, CA). The data discussed in this publication have been deposited in NCBI's Gene Expression Omnibus [29] and are accessible through GEO Series accession number GSE37842 (http://www.ncbi.nlm.nih.gov/geo/query/acc.cgi?acc = GSE37842).

Karyotype Analysis

Cells were cultured with colcemid (0.06 μg/ml; Invitrogen) at 37°C for 4 hours, and single-cell suspensions were prepared by 0.05% trypsin/EDTA dissociation after pre-treatment with Y-27632 to prevent apoptosis. After incubation in 75 mM KCl for 20 min, the cells were fixed in Carnoy fluid. The fixed samples were heat-denatured at 95°C for 2 hours, incubated in 0.025% trypsin for 10 sec, and stained with Giemsa (Merck, Darmstadt, Germany) for 7 min. The samples were observed under a microscope (Carl Zeiss), and metaphase samples were analyzed using Ikaros (MetaSystems, Altlussheim, Germany).

Genotyping of Short Tandem Repeat (STR) Polymorphisms

Genomic DNA was extracted by DNAzol Reagent (Invitrogen). STR loci were investigated with the Powerplex 16 system (Promega, Madison, WI) using an ABI PRISM 3100 Genetic Analyzer (Applied Biosystems) and analyzed by GeneMapper software (Applied Biosystems) following the manufacturer's instructions [26].

Bisulfite Modification and DNA Sequencing

Genomic DNAs were bisulfite-treated with the EZ DNA methylation-Gold Kit (ZYMO Research, Orange, CA), according to the manufacturer's instructions. The human OCT4 and NANOG promoter regions were amplified with specific primer sets (Supplemental Table S2) by TaKaRa Taq™ Hot Start Version (Takara Bio INC., Shiga, Japan). The PCR products were sub-cloned into the p2.1 vector (Invitrogen). Ten clones were sequenced with a universal primer by ABI PRISM 3100 Genetic

Analyzer (Applied Biosystems) and analyzed by Sequence analysis software (Applied Biosystems), following the manufacturer's instructions.

In vitro Differentiation Assay

Cells were incubated with collagenase type IV (1 mg/ml; Invitrogen) for 3 min at 37°C and harvested by scraper. The harvested colonies were then incubated on petri dishes in hESC medium without bFGF to form embryoid bodies (EBs). After 8 days of floating culture, the EBs were harvested for transcript analysis. Some of the EBs were transferred to gelatin-coated chamber slides (Nunc, Roskilde, Denmark) and cultured for another week (total 15 days) in DMEM supplemented with 10% FBS, at 37°C in 5% CO_2 [1].

Teratoma Formation Assay

NOG (NOD/Shi-scid IL2Rgnull) mice [30] aged 6–8 weeks were maintained under specific-pathogen-free conditions in the Animal Facility of the Central Institute for Experimental Animals (CIEA). All mice studies were carried out in accordance with the guidelines of the Animal Care Committee at CIEA and approved by the Animal Care Committee at CIEA. The recipient mice were anesthetized by isoflurane inhalation (Dainippon Pharmaceutical Co., Ltd., Osaka Japan). Human iPSCs were xeno-transplanted into both subcutaneous tissues and kidney capsules. For subcutaneous transplantation, hiPSCs (1×10^6 cells/0.1 ml of serum-free medium) were subcutaneously inoculated into the flank. For transplantation into the kidney capsule, the kidney was exteriorized through a dorsal-horizontal incision. A syringe with a 29G needle with a flattened tip was introduced into the kidney at a site away from the transplanted region. The kidney was penetrated, the tip of the needle positioned just beneath the renal capsule, and then the cell suspension of hiPSCs (1×10^5 cells/10 µl of serum-free medium) was then injected underneath the kidney capsule. The mice were examined daily, and tumors were measured with calipers. The teratoma samples were resected and fixed with 4% (v/v) phosphate-buffered formalin, and paraffin-embedded sections were stained using with hematoxylin and eosin (H&E staining) according to standard procedures.

Immunocytochemical Staining

Cells were fixed in 4% PFA and washed with PBS. The fixed samples were permeabilized with 0.1% Triton X-100, blocked with 10% normal goat serum, and then reacted with the following Abs overnight at 4°C: anti-α-fetoprotein (AFP) Ab (SantaCruz, Santa Cruz, CA), anti-Cytokeratin19 Ab (clone A53-B/A2, Santa Cruz), anti-Desmin Ab (Thermo, Waltham, MA), anti-α-smooth muscle actin (SMA) Ab (clone 1A4, Dako, Carpinteria, CA), anti-glial fibrillary acidic protein (GFAP) Ab (Sigma, St. Louis, MO), anti-βIII-tubulin Ab (clone TuJ1, Babco, Richmond, CA), anti-OCT3/4 Ab (Chemicon), and anti-NANOG Ab (Reprocell, Tokyo, Japan). After several washes, the samples were incubated with the appropriate secondary Abs (AlexaFluor®-488-conjugated goat anti-mouse IgG Ab, AlexaFluor®-568-conjugated goat anti-rabbit IgG Ab, Molecular Probes, Invitrogen), and TO-PRO-3® iodide (1 mM, Molecular Probes, Invitrogen) for 1 hour at RT.

The samples were examined using a confocal laser scanning microscope (LSM510, Carl Zeiss, Hallbergmoos, Germany). All stainings were performed with matched isotype controls.

Statistical Analysis

Statistical differences in the number of hESC-like colonies were determined by the Kruskal-Wallis test, and differences in gene expression levels obtained by qRT-PCR were determined by unpaired Student's t-tests or ANOVA with post-hoc comparisons. Details are given in the figure legends.

Results

Generation of hiPSCs on PCM-DM

First, we examined the feasibility of generating hiPSCs on PCM-DM. After transducing DMCs with the four Yamanaka factors (OSKM) by retroviruses, the DMCs were seeded on PCM-DM and cultured with MEF-CM (Fig. 1A). After 30 days of induction, the hESC-like colonies were picked up, replated on PCM-DM (passage 1), the culture medium was changed to StemPro medium (passage 2), and the cells were further propagated (Fig. 1A). Among the colonies, we selected two representative hiPSC-PCMDM clones (clone 1, iPS-DMC72-PCMDM01; clone 2, iPS-DMC72-PCMDM02), which had an hESC-like morphology, characterized by large nuclei, scant cytoplasm, and flat-dense colonies, and analyzed their pluripotent stem cell properties in detail at early (about passage 10) and late (after passage 20) culture times.

Characterization of hiPSC-PCMDM at Early and Late Culture Times

The two established hiPSC-PCMDM clones showed good proliferation activity, and retained their hESC-like morphology and ALP activity at the early and late passages (Fig. 1B, C). Expression analysis of the four transgenes OSKM by qRT-PCR showed that the mRNA copy number of each was well suppressed at the early and late culture times, in contrast to day 3 after infection (Fig. 2A). To examine the endogenous expression of OSKM and NANOG, we quantified their transcript level by qRT-PCR and compared it to the level in hESCs (KhES1) (Fig. 2B). Although the SOX2, c-MYC, and NANOG expression tended to be lower in the hiPSC-PCMDM clones than in KhES1, all these undifferentiated marker genes were expressed within an acceptable range of variation in the two hiPSC-PCMDM clones (Fig. 2B).

To examine the protein levels of hESC-marker molecules, we analyzed the two established clones by immunocytochemistry and FCM. Immunocytochemistry showed that the two clones stably expressed both OCT4 and NANOG in their nuclei at the early and late culture times (Fig. 2C). FCM analysis revealed that the clones highly expressed hESC-specific surface antigens (SSEA-3, SSEA-4, TRA-1-60, and TRA-1-81), at levels that were similar to KhES1 and stable between the early and late culture times (Fig. 2D). These findings indicated that the two established hiPSC-PCMDM clones were almost identical to hESCs in their undifferentiated state, and that their cellular properties were highly stable over long periods in culture.

In vitro Differentiation

The in vitro pluripotency of the two hiPSC-PCMDM clones was examined by EB formation assay. After 8 days of culture in petri dishes without bFGF, both clones formed EBs, whether the cells were taken from the early or late passages (Fig. 3A). Quantitative RT-PCR analysis showed that the OCT4 and TERT expressions were generally lower after EB formation than before, in both clones (Fig. 3B). NANOG expression was also suppressed in clone 1 (early and late passages); however, it was not markedly suppressed in clone 2 at either passage (Fig. 3B).

The expressions of lineage-specific (endoderm, mesoderm, and ectoderm) marker genes after the 8 days of EB formation were examined by qRT-PCR analysis and compared with those of differentiated hiPSCs (201B7) [1]. The expression levels of nine

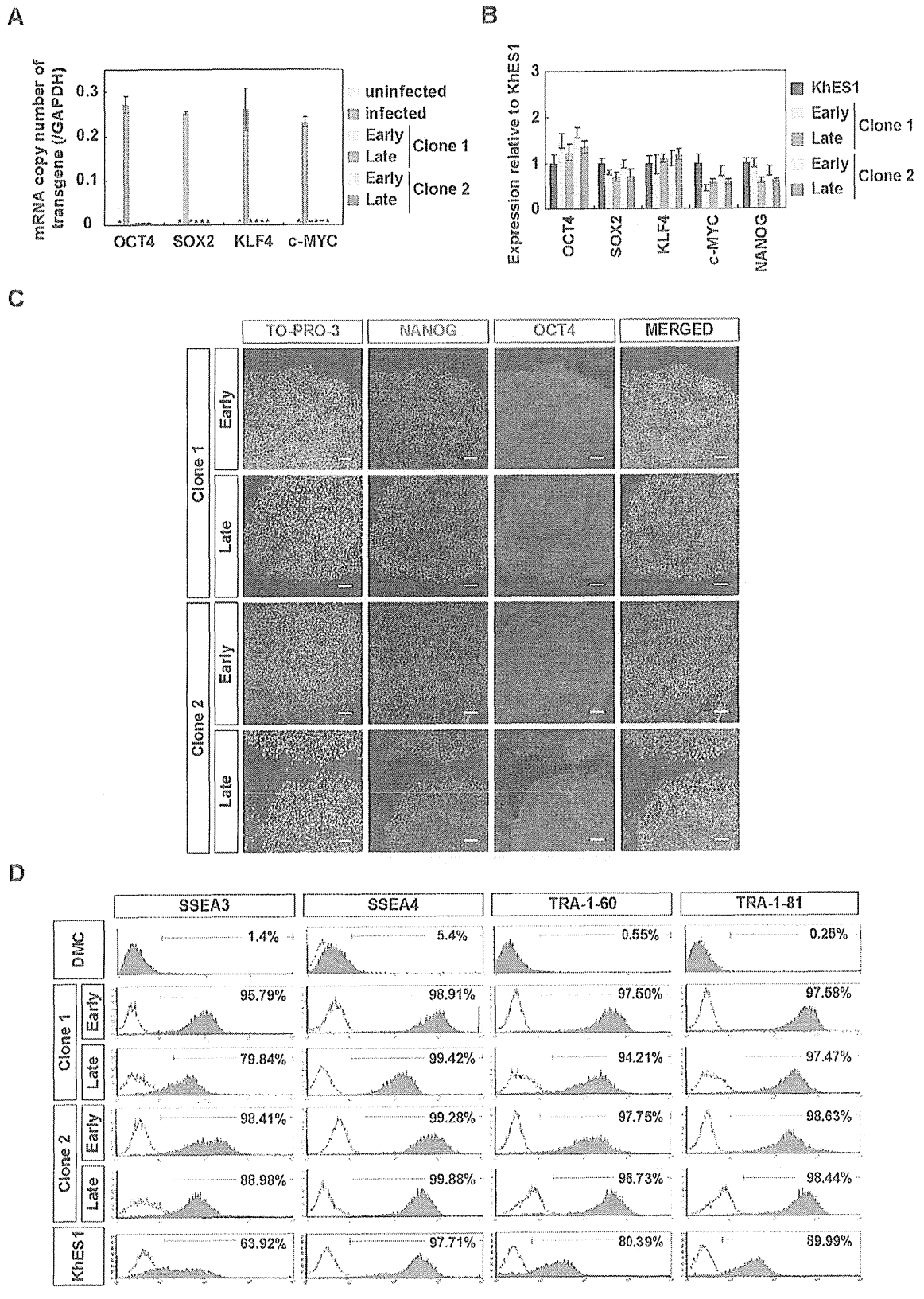
A
mRNA copy number of transgene (/GAPDH)
0.3
0.2
0.1
0
OCT4
SOX2
KLF4
c-MYC
uninfected
infected
Early
Late
Clone 1
Early
Late
Clone 2
B
Expression relative to KhES1
3
2
1
0
OCT4
SOX2
KLF4
c-MYC
NANOG
KhES1
Early
Late
Clone 1
Early
Late
Clone 2
C
TO-PRO-3
NANOG
OCT4
MERGED
Clone 1
Early
Late
Clone 2
Early
Late
D
SSEA3
SSEA4
TRA-1-60
TRA-1-81
DMC
1.4%
5.4%
0.55%
0.25%
Clone 1
Early
95.79%
98.91%
97.50%
97.58%
Late
79.84%
99.42%
94.21%
97.47%
Clone 2
Early
98.41%
99.28%
97.75%
98.63%
Late
88.98%
99.88%
96.73%
98.44%
KhES1
63.92%
97.71%
80.39%
89.99%

Figure 2. In vitro characterization of hiPSCs generated on PCM-DM. A) Quantitative RT-PCR analysis for the mRNA copy number of four transgenes (OCT4, SOX2, KLF4, c-MYC). All the transgenes were silenced in two hiPSC-PCMDM clones. Data are presented as the mean ± SD. Clone 1, iPS-DMC72-PCMDM01; Clone 2, iPS-DMC72-PCMDM02; Early, passage 8; Late, passage 30; *: not detected. B) Quantitative RT-PCR analysis for hESC marker gene (OCT4, SOX2, KLF4, c-MYC, NANOG) expression at early (passage 8) and late (passage 30) culture times compared with hESCs (clone KhES1). Data are presented as the mean ± SD. C) Immunocytochemistry for NANOG (red) and OCT4 (green) expression in hiPSC-PCMDM clones. Clone 1, Early (passage 10), Late (passage 22); Clone 2, Early (passage 11), Late (passage 25). Scale bar = 200 μm. D) Flow cytometry analysis for hESC-specific surface antigens (SSEA-3, SSEA-4, TRA-1-60, and TRA-1-81) at early (passage 10) and late (passage 30) culture times in comparison with parental DMCs and hESCs (KhES1). Clone 1, iPS-DMC72-PCMDM01; Clone2, iPS-DMC72-PCMDM02.
doi:10.1371/journal.pone.0055226.g002

marker genes in EBs were equivalent to or higher than those in differentiated 201B7 regardless of the clone or culture time (Fig. 3B). To confirm the progression of differentiation, we cultured the EBs on gelatin-coated chamber slides for 8 days, and then with 10% FBS-containing medium for an additional week. After this 15-day total in vitro differentiation, the samples were examined by immunocytochemistry. At this point, the cells in the EBs had differentiated into various adherent cells, most of which expressed little OCT4 or NANOG (Fig. 3C). Some of these adherent cells expressed endoderm (AFP or cytokeratin), mesoderm (desmin or α-SMA), or ectoderm (GFAP or βIII-tubulin) marker proteins (Fig. 3C). These results indicated that the two established hiPSC-PCMDM clones had in vitro pluripotency, which was stably maintained in feeder-free culture on PCM-DM for over 20 passages.

Karyotyping, Genotyping, and Promoter Methylation Analyses

Karyotyping by G-band staining showed that both hiPSC-PCMDM clones had a normal female karyotype (46, XX) at the early and late culture times (Fig. 4A). Analysis of the methylation states of the OCT4 and NANOG promoter regions revealed that most of the CpG sites were unmethylated in the two hiPSC-PCMDM clones; in contrast, those of the parental DMCs were highly methylated (Fig. 4B). Genotyping by STR-PCR showed that the STRs completely matched between the parental DMCs and the two established clones (Supplemental Table S3). These findings showed that the two hiPSC-PCMDM clones were derived from the parental DMCs, and that their epigenetic states appeared to be reprogrammed efficiently. Furthermore, their karyotypes remained normal in the feeder-free culture on PCM-DM for over 20 passages.

Teratoma Formation from hiPSC-PCMDM Clones at Early and Late Passages

The pluripotency of the two clones was also evaluated by *in vivo* teratoma formation assay. Both clones, whether cultured for short or longer times, equally formed tumor masses in NOG mice after several months, and these masses contained various histological components of the three germ layers. The tumors partly showed neural rosette-like structures (ectoderm), cartilage-like structures (mesoderm), or gut-like epithelium (endoderm) (Fig. 5). These findings indicated that both hiPSC-PCMDM clones could form teratomas showing in vivo pluripotency, and that their in vivo pluripotency was fully preserved after feeder-free culture on PCM-DM for over 20 passages. Collectively, these findings confirmed that the two established hiPSC-PCMDM clones met the criteria for hiPSCs, and thus, the feeder-free generation and long-term maintenance of hiPSCs on PCM-DM was successful.

Global Gene Expression of hiPSC-PCMDM

To further characterize the hiPSC-PCMDM clones at the molecular level, we examined their genome-wide gene-expression profiles and compared them with those of hESCs (KhES1) and hiPSCs (201B7). Microarray analysis showed that the global gene expression profiles of the hiPSC-PCMDM clones at early and late passages were very similar, and that the differences between the two clones were very small (Fig. 6A). However, some gene expressions changed over time (Fig. 6A, B). When we focused on the expressions of a stem cell marker gene set suggested by the International Stem Cell Initiative [31], some genes (clone 1: fibroblast growth factor 4 [FGF4] and undifferentiated embryonic cell transcription factor 1 [UTF1]; clone 2: growth differentiation factor-3 [GDF3]) were more highly expressed at the late passage (Fig. 6A, Supplemental Table S4). On the other hand, the expression of the X (inactive)-specific transcript (non-protein coding) gene (XIST) in hiPSC-PCMDM clone 1 was markedly suppressed at late passages, to the level seen in hiPSC-PCMDM clone 2 (Fig. 6A, Supplemental Table S4). Moreover, comparison of the gene expression of the hiPSC-PCMDM clones with that of KhES1 or 201B7 showed that GATA-binding factor 6 (GATA6) was more highly expressed in both clones than in KhES1 or 201B7 from the early passage (Fig. 6A); these results were confirmed by qRT-PCR analysis (Fig. 6B).

Finally, cluster analysis showed that the two hiPSC-PCMDM clones were clearly separated from the parental DMCs and the clusters of KhES1 and 201B7 (Fig. 6C). Interestingly, the clones from the early passage and late passage also clustered separately. These results indicate that the gene-expression patterns of the hiPSC-PCMDM clones were similar to those of KhES1 and 201B7 but not to those of the parental DMCs. Moreover, the differences in the established hiPSC-PCMDM clones between the early and late passages were relatively small, but they trended similarly as the number of passages increased.

Expression of GATA6 in hiPSC-PCMDM

The factors affecting GATA6 gene expression were also examined. An established iPSC clone (201B7), which was routinely propagated on SNL feeder cells and in hESC medium, was reseeded on PCM-DM using MEF-CM or StemPro medium, and the gene expressions of OCT4 and GATA6 were examined for 3 passages (Fig. 7A, B). OCT4 expression was almost the same under both culture conditions (Fig. 7A). In contrast, GATA6 expression was significantly up-regulated in the cells cultured in StemPro medium and was not expressed in those cultured in MEF-CM (Fig. 7A). These findings indicated that the GATA6 expression might be induced by the StemPro medium and not by PCM-DM.

Reprogramming Efficiency Using PCM-DM Versus Other Substrates

We also established hiPSC clones (iPS-DMC71-PCMDM and iPS-DMC92-PCMDM) by the same method, using PCM-DM with MEF-CM. These two clones had a clear hESC-like morphology and ALP activity (Supplemental Figure S1A). Expression analysis by qRT-PCR showed that the mRNA copy number of the four transgenes OSKM was fully suppressed (Supplemental Figure S1B) and that the endogenous expression levels of OSKM and NANOG

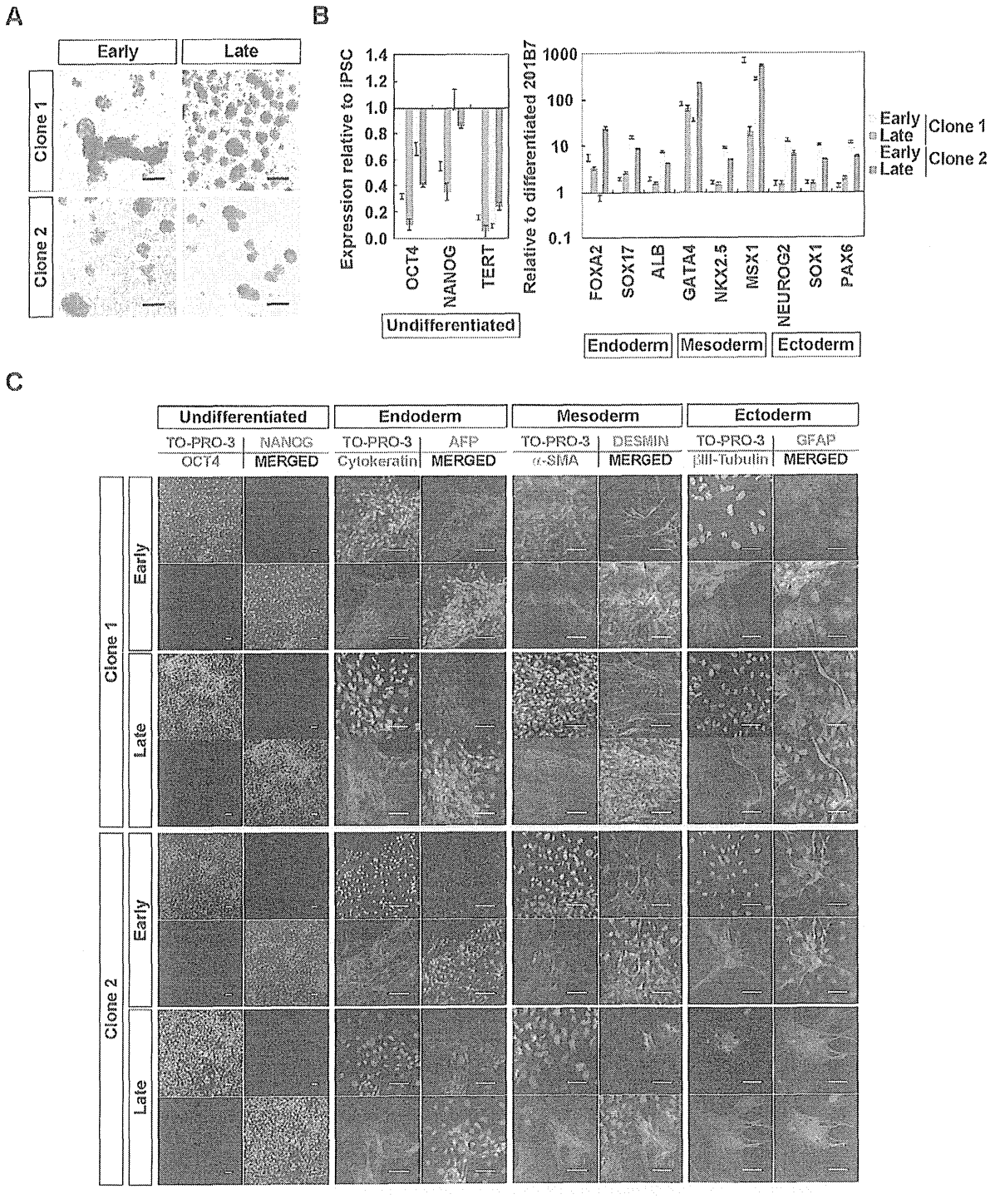

Figure 3. In vitro differentiation of hiPSCs generated on PCM-DM at early and late passages. A) Embryoid bodies (EBs) on day 8, derived from hiPSCs generated on PCM-DM at early (Clone 1, passage 11; Clone 2, passage 12) and late (Clone 1, passage 22; Clone 2, passage 21) culture times. Scale bar = 200 μm. B) Quantitative RT-PCR analysis. Left: Expression levels of undifferentiated genes in EBs relative to the hiPSCs before differentiation. Right: Expression levels of lineage-specific genes in EBs relative to differentiated 201B7. Data are presented as the mean ± SD. C) Immunocytochemical staining of differentiated cells by culturing EBs on gelatin-coated chamber slides with DMEM containing 10% FBS for 1 week. Clone 1, iPS-DMC72-PCMDM01; Clone 2, iPS-DMC72-PCMDM02. Scale bar = 50 μm.
doi:10.1371/journal.pone.0055226.g003

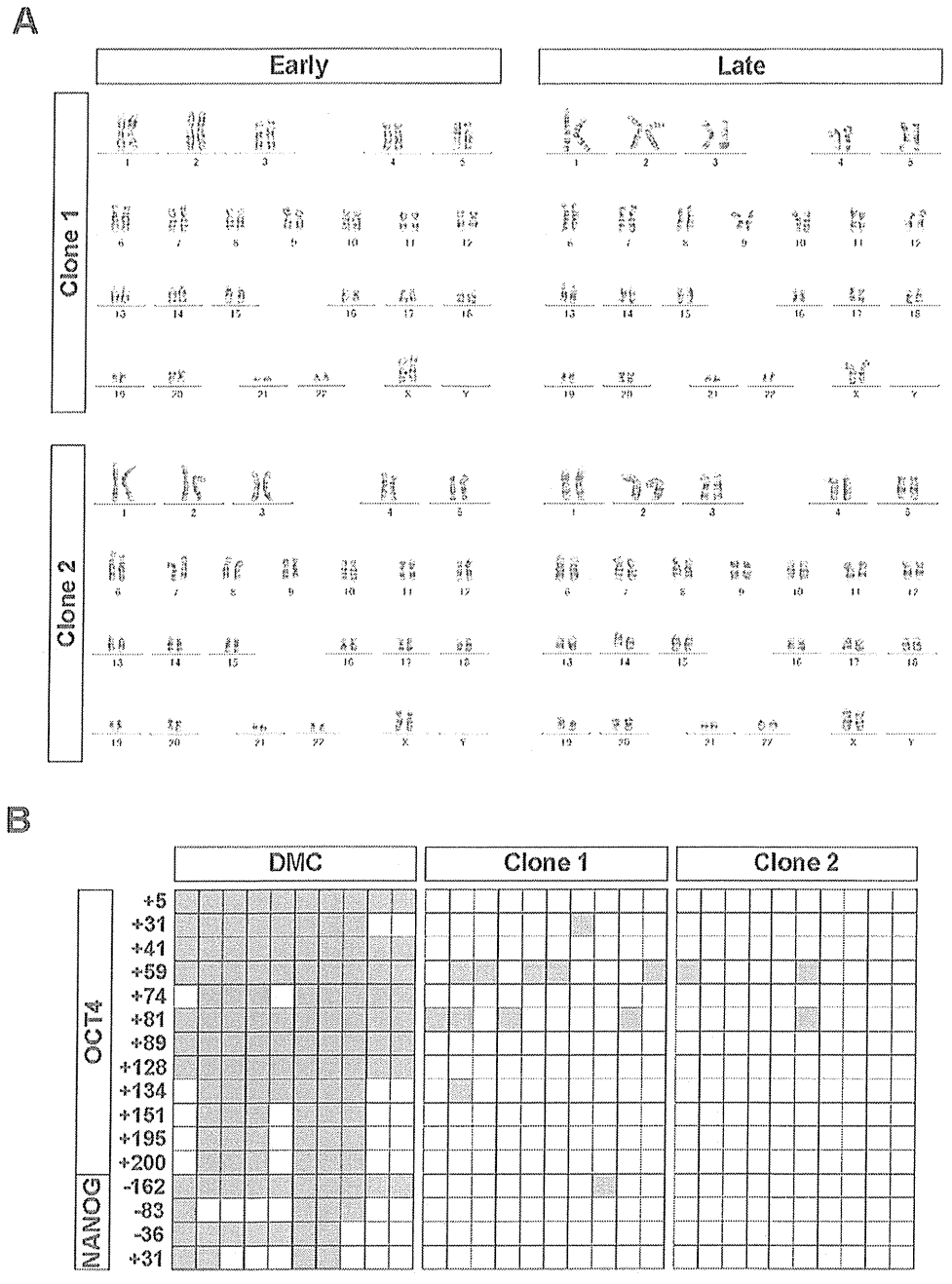

Figure 4. Karyotype and promoter methylation analyses of hiPSCs generated on PCM-DM. A) G-band staining of the two hiPSC-PCMDM clones showing a normal female karyotype (46, XX) in both clones at early (Clone 1, passage 12; Clone 2, passage 12) and late (Clone 1, passage 23; Clone 2, passage 24) passages. B) Methylation states of the OCT4 and NANOG promoter of the two hiPSC-PCMDM clones (passage 29) using bisulphate sequencing. Numbers indicate the position from the transcription start site. Open squares indicate unmethylated and filled squares indicate methylated CpG dinucleotides. Clone 1, iPS-DMC72-PCMDM01; Clone 2, iPS-DMC72-PCMDM02.
doi:10.1371/journal.pone.0055226.g004

were within the acceptable range of variation, compared with the level in hESCs (Supplemental Figure S1C). Immunocytochemistry showed that the two clones stably expressed both OCT4 and NANOG in their nuclei (Supplemental Figure S1D). These findings showed that the feeder-free generation and culture of hiPSCs using PCM-DM is feasible and reproducible.

To examine the applicability of iPSC generation using PCM-DM further, we compared the reprogramming efficiency for six different lines of DMCs under seven different culture conditions as follows: plated on MEFs with NC-hESC medium (control), on PCM-DM with MEF-CM, on Matrigel with MEF-CM, on gelatin with MEF-CM, on PCM-DM with NC-hESC medium, on Matrigel with NC-

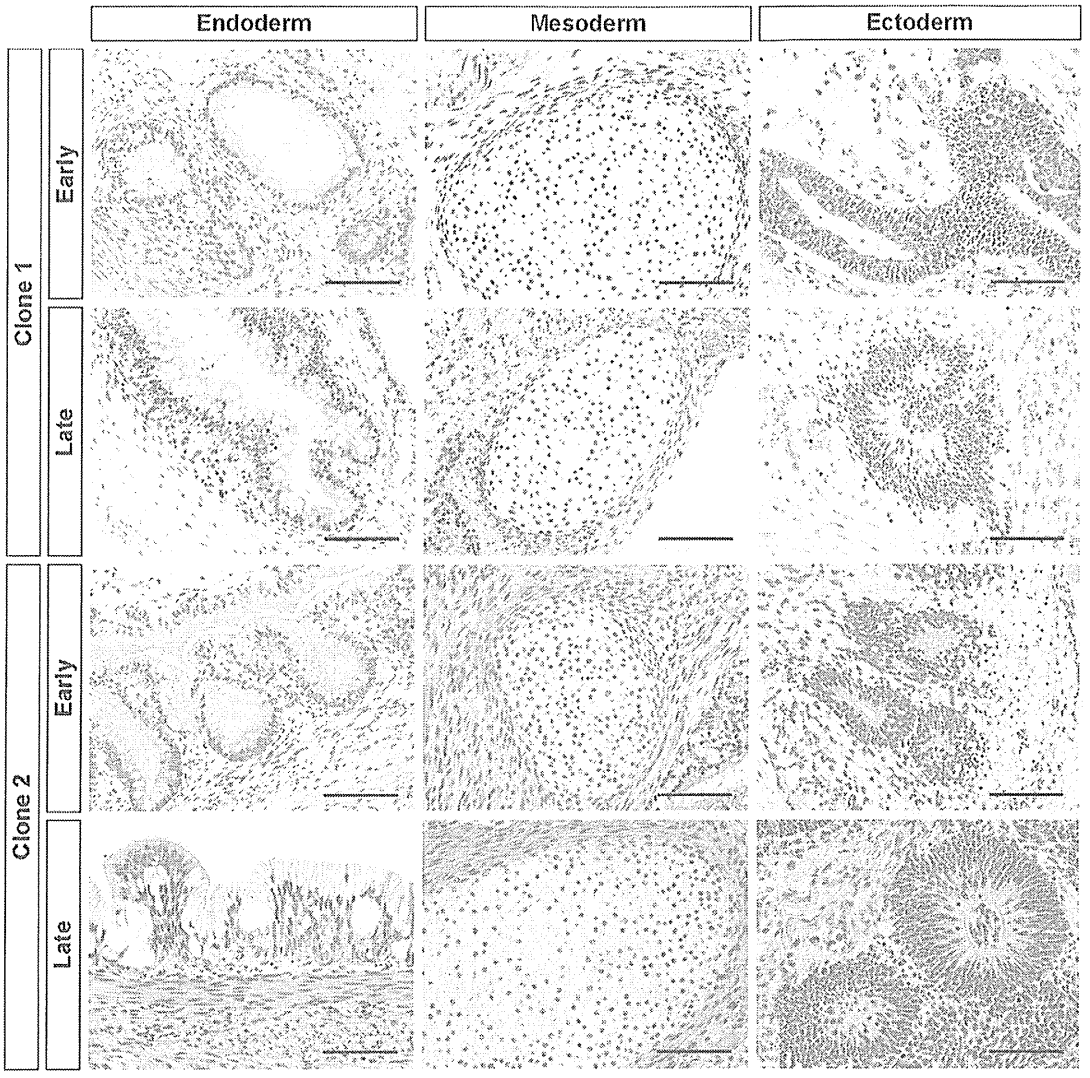

Figure 5. In vivo differentiation of hiPSCs generated on PCM-DM at early and late passages. hiPSC-PCMDM-induced teratomas were excised from mice and processed for H&E staining. Clone 1, iPS-DMC72-PCMDM01; Clone 2, iPS-DMC72-PCMDM02. Early, passage 12; Late, passage 23; Scale bar = 100 μm.
doi:10.1371/journal.pone.0055226.g005

hESC medium, and on gelatin with NC-hESC medium. In the cultures with MEF-CM, the most hESC-like colonies appeared on Matrigel, with a statistically significant efficiency; fewer, but still significant, numbers of hESC-like colonies were also obtained using PCM-DM or gelatin (Fig. 8, Supplemental Table S5). On the other hand, in the cultures using NC-hESC medium, we obtained hESC-like colonies at lower levels, with similar efficiencies, on PCM-DM and Matrigel (Fig. 8, Supplemental Table S5). In contrast, no colonies with clear hESC-like characteristics were obtained from DMCs cultured on gelatin with NC-hESC medium (Fig. 8, Supplemental Table S5). These findings suggest that PCM-DM could be used to generate hiPSCs with a reprogramming efficiency that was almost as good or the same as that of other substrates used with MEF-CM or NC-hESC medium.

Cellular Properties of hiPSCs Generated on PCM-DM in Non-conditioned Medium

Finally, to examine the applicability of hiPSCs generated on PCM-DM without MEF-CM, we examined the detailed cellular properties of hiPSCs generated on PCM-DM in NC-hESC medium. One representative clone (iPS-DMC75-PCMDM), which was initially reprogramed on PCM-DM with NC-hESC medium and further propagated on PCM-DM with StemPro medium after 2 passages, retained its hESC-like morphology and had ALP activity (Fig. 9A). Expression analysis of the four transgenes OSKM by qRT-PCR showed that the mRNA copy number of each was suppressed (Fig. 9B). Immunocytochemistry showed that this clone stably expressed both OCT4 and NANOG in its nuclei (Fig. 9C). FCM analysis revealed that this clone highly expressed hESC-specific surface antigens (SSEA-3, SSEA-4, TRA-1-60, and TRA-1-81) (Fig. 9D), and microarray analysis showed

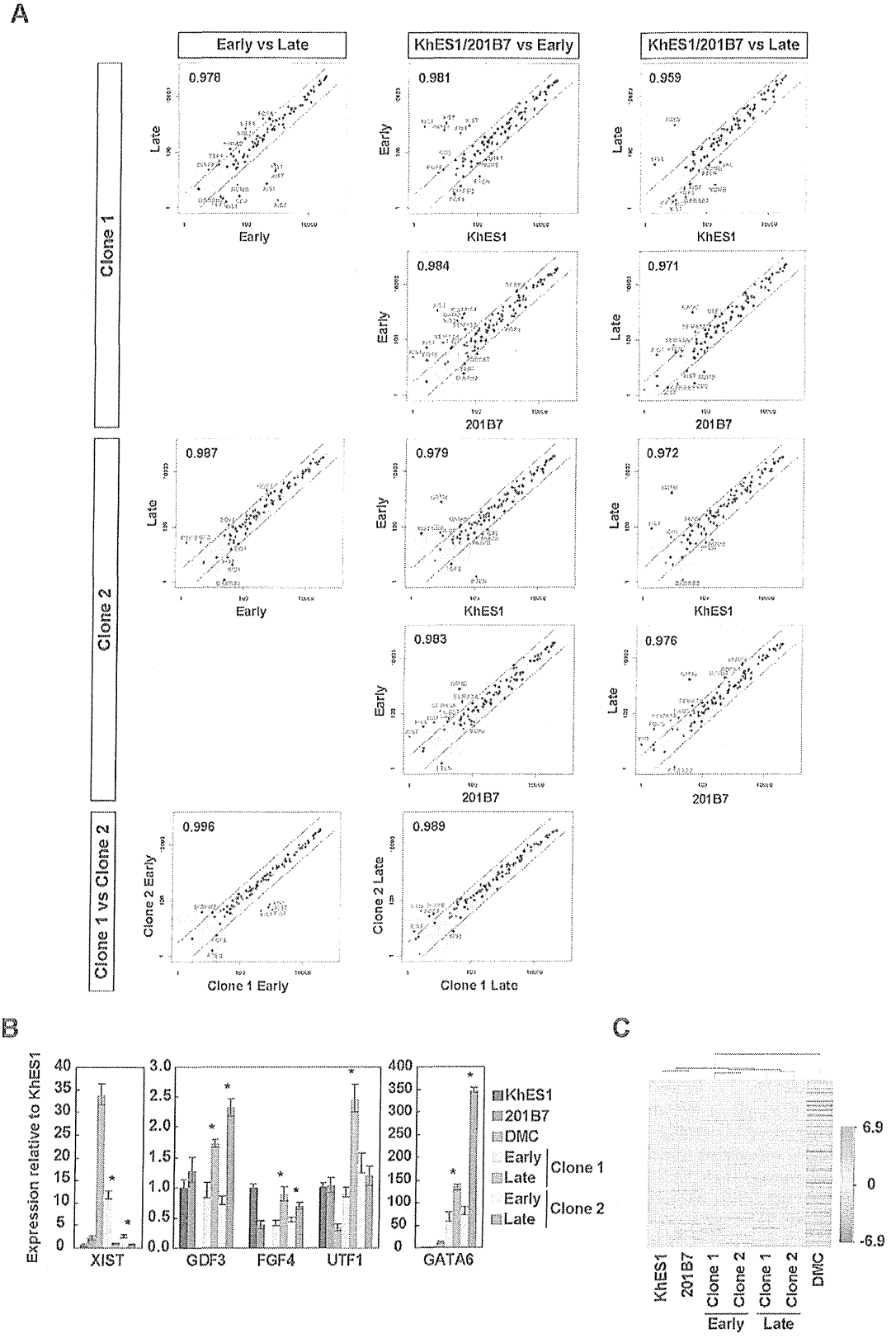
A
Early vs Late
KhES1/201B7 vs Early
KhES1/201B7 vs Late
Clone 1
Clone 2
Clone 1 vs Clone 2
0.978
0.981
0.959
0.984
0.971
0.987
0.979
0.972
0.983
0.976
0.996
0.989
Late
Early
KhES1
201B7
Clone 2 Early
Clone 1 Early
Clone 2 Late
Clone 1 Late
B
Expression relative to KhES1
XIST
GDF3
FGF4
UTF1
GATA6
KhES1
201B7
DMC
Early
Late
Clone 1
Clone 2
C
6.9
0
-6.9
KhES1
201B7
Clone 1
Clone 2
Clone 1
Clone 2
DMC
Early
Late

Figure 6. Global gene expression analysis. A) Global gene expression of the hiPSC-PCMDM clones, KhES1, and 201B7 by microarray analysis. Scatter plots and Pearson's coefficient are shown. The diagonal lines indicate 3-fold changes in gene expression levels. Plus ("+") symbols indicate stem-cell marker genes suggested by the International Stem Cell Initiative [31], and such genes outside the 3-fold change lines are shown in red text. Early, passage 8; Late, passage 30. Clone 1, iPS-DMC72-PCMDM01; Clone 2, iPS-DMC72-PCMDM02. B) Quantitative RT-PCR analysis of the XIST, GDF3, FGF4, UTF1, and GATA6 genes. Data are presented as the mean ± SD. Early, passage 8; Late, passage 30. Statistical differences between early and late passage group are determined by unpaired Student's t-test (*, $P<0.01$). C) Hierarchical cluster analysis between parental DMCs, KhES1 cells, 201B7, and the two hiPSC-PCMDM clones at early (passage 8) and late (passage 30) passages.
doi:10.1371/journal.pone.0055226.g006

that its global gene expression patterns were similar to the early and late passages of clones 1 and 2, as well as to KhES1 and 201B7 (Fig. 9E). Moreover, iPS-DMC75-PCMDM expressed GATA6 at a higher level than KhES1 or 201B7, and at about the same level as clones 1 and 2 (Fig. 9E). This clone formed EBs (Fig. 9F) and differentiated into the three germ layers, as assessed on the gene expression level (Fig. 9G), although the expression of the undifferentiated marker NANOG persisted for 8 days after the start of differentiation. These findings show that it is feasible to generate hiPSCs on PCM-DM without MEF-CM.

Discussion

Feeder-cell-free Generation of hiPSCs on PCM-DM

It is easier to control the quality of feeder-cell-free cultures than of those that use human-derived primary cells, which makes them more attractive for clinical applications. In general, the characteristics of human-derived primary cells (e.g., dermal fibroblasts) that are used for xenobiotic-free culture methods vary widely from line to line, and can only be passaged a small number of times. Moreover, their feeder-cell activity for hiPSCs/hESCs can vary from batch to batch [27]. To overcome these variabilities, various xenobiotic- and feeder-cell-free methods have been developed. Of these, Matrigel [6–9] has been widely used as a standard control. In addition to Matrigel, several other materials, including laminin-511 [14,15], fibronectin [10–13], vitronectin [32–35], collagen I [36], and E-cadherin [37] exhibit maintenance activity for hiPSCs/hESCs, and fibronectin was reported to support hiPSC generation [10]. More complex and mixed materials like human-serum matrix [38], human fibroblast extracellular matrix [39,40], and autologous extracellular matrix (from H9 EB derived-cells) [41] are also reported to be useful for culturing hiPSCs/hESCs.

In this study, we examined PCM-DM as a feeder-cell-free method for generating hiPSCs, because it is a human-derived material with the ability to maintain hiPSCs/hESCs equivalent to that of Matrigel [23]. Human iPSCs generated on PCM-DM showed clear hESC-compatible phenotypes in their undifferentiated state, and they differentiated into three germ layers in vitro and in vivo. These hESC-like properties of hiPSC-PCMDM were fully maintained for at least 20 passages, and detailed analysis using microarrays showed that the global gene expression profiles of the hiPSC-PCMDM clones were also quite stable over 20 passages (Fig. 6). Moreover, we succeeded in establishing additional hiPSC clones (iPS-DMC71-PCMDM and iPS-DMC92-PCMDM) by the same method, using PCM-DM with MEF-CM, and these clones also had hESC-like properties (Supplemental Fig. S1). These findings indicated that the generation and long-term maintenance of hiPSCs on PCM-DM, with no exposure to feeder cells, is feasible and reproducible, and that the cell biological properties of the hiPSCs are well retained on PCM-DM.

Although we have not yet identified the molecular components of PCM-DM responsible for supporting the self-renewal and pluripotency of the hiPSCs/hESCs because of its complexity, PCM-DM is reported to include fibronectin and collagen IV but very little laminin [23]. Therefore, the properties of PCM-DM may be different from laminin-based materials such as Matrigel, which is mainly composed of laminin-111, or human recombinant laminin-511 [14,15]. PCM-DM and Matrigel, which is also complex, show higher activity for maintaining hESCs than their individual components such as fibronectin [11,23]; of these, PCM-DM as a human-derived material may be more useful for medical applications.

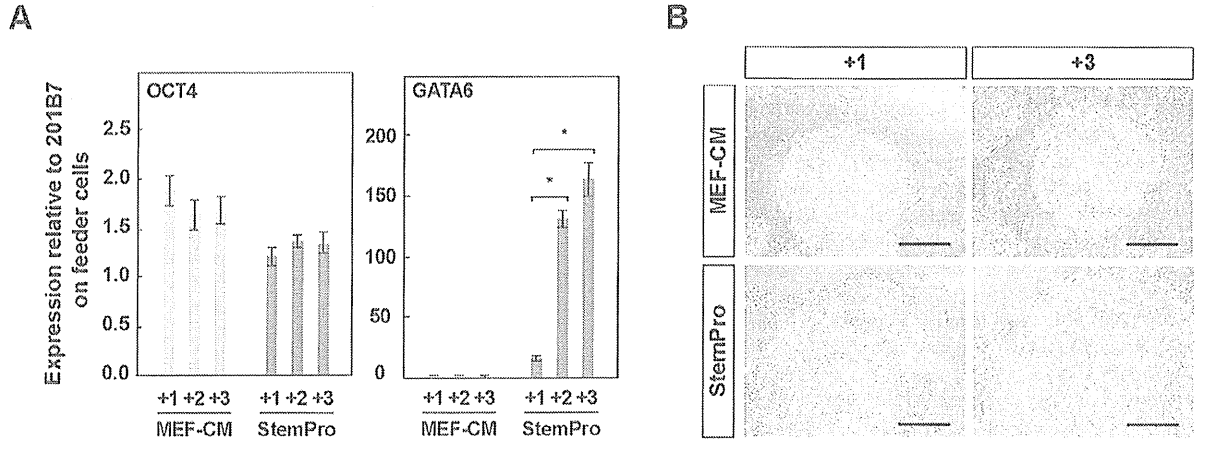

Figure 7. Increased GATA6 expression in 201B7 on PCM-DM with StemPro medium. A) Quantitative RT-PCR analysis of OCT4 and GATA6 for 201B7 cultured on PCM-DM with MEF-CM or StemPro medium. "+number" indicates the passage number after reseeding on PCM-DM. Statistical significances are determined by Scheffe's test after two-way ANOVA. Results of comparisons among groups of medium within each passage are shown (*, $P<0.01$). B) Morphology of 201B7 cultured on PCM-DM with MEF-CM or StemPro medium. Scale bar = 500 μm.
doi:10.1371/journal.pone.0055226.g007

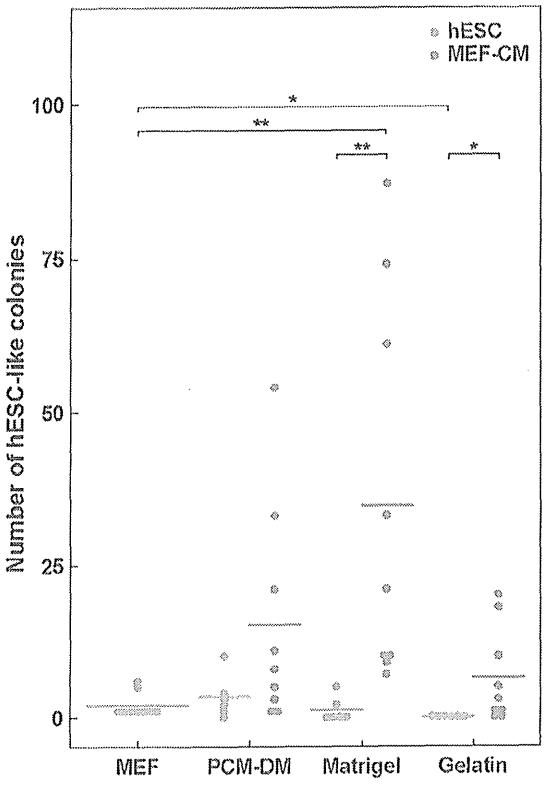

Figure 8. Comparison of reprogramming efficiency. Number of hESC-like colonies derived from DMCs under seven different conditions: MEF with hESC medium, PCM-DM with NC-hESC medium, Matrigel with NC-hESC medium, gelatin with NC-hESC medium, PCM-DM with MEF-CM, Matrigel with MEF-CM, and gelatin with MEF-CM. Horizontal bars indicate the mean for each method. Statistical differences were determined by the Kruskal-Wallis test (*, $p<0.05$, **, $P<0.01$).
doi:10.1371/journal.pone.0055226.g008

Gene Expression Properties of hiPSC-PCMDM

The cellular properties of the hiPSC-PCMDM clones were almost identical to those of hiPSCs generated and maintained on feeder cells; however, some interesting differences were found. We found higher expression levels of FGF4 and UTF1 in clone 1 and of GDF3 in clone 2 at the late passage. FGF4 and UTF1 are target genes of OCT4 and SOX2 [42,43]. In our study, the OCT4 and SOX2 expressions were almost unchanged between the early and late passages in both clones (Fig. 2B), and FGF4 and UTF1 showed only small changes when compared with KhES1 (Fig. 6B). We think that these differences in FGF4 and UTF1 expression seen in clone 1 were acceptable dispersion that is unlikely to significantly affect the cellular properties of clone 1. GDF3 has been identified in Activin-treated embryonic carcinoma cells, and it contributes to the maintenance of hESCs [44–46]. In this study, starting at passage 2, we used the StemPro medium, which contains Activin (10 ng/ml) and might gradually induce GDF3 over time in culture, although MEF-CM also contains Activin [47].

In contrast, XIST was more highly expressed in clone 1 at the early passage than in KhES1 or 201B7. The expression level of XIST, which is involved in the inactivation of chromosome X in female cells, appeared to decrease gradually toward the level in KhES1 and 201B7 with long-term culture. A high expression level of XIST in DMCs is reasonable, because DMCs are female-derived cells and XIST helps elicit the dosage compensation for chromosome X [48]. Given that KhES1 and 201B7 are also female-derived cells and showed low XIST expression, and some female hiPSCs [49] and hESCs [50–53] are reported to show decreasing expression of XIST during culture, our hiPSC clones may resemble good hiPSCs in this respect. That is, the decreased XIST expression in female hiPSCs and hESCs may indicate a global epigenetic status that is specific for pluripotent stem cells [49].

In addition to XIST, interestingly, GATA6 was more highly expressed in our two established clones than in KhES1 or 201B7 throughout the long culture period. GATA6 is considered to be a marker for primitive or definitive endoderm in early embryogenesis [54,55]. Although the hiPSC-PCMDM clones showed full pluripotency as a mass both in vitro and in vivo, the expression of GATA6 in hiPSC-PCMDM might indicate that some cells spontaneously differentiated into extra-embryonic tissues or definitive endoderm. On the other hand, our examinations using 201B7 showed that the GATA6 expression in hiPSCs cultured on PCM-DM was completely repressed by MEF-CM, but not by StemPro medium. This finding indicated that the GATA6 expression may be induced by the StemPro medium, not by the PCM-DM itself.

StemPro medium is a defined culture medium developed for hiPSCs/hESCs; it contains Activin A, FGF2, ErbB-2 ligand HRG-1 beta, and insulin-like growth factor ligand LR3-IGF1 [56]. We previously confirmed that the combination of StemPro medium and PCM-DM was useful for maintaining hiPSCs/hESCs [23]. Activin can induce the differentiation of definitive endoderm from hESCs [57]. Although Activin is also present in MEF-CM, McLean et al reported that hESCs cultured with MEF-CM and Matrigel could differentiate into definitive endoderm only when the phosphatidylinositol 3-kinases (PI3K) signaling pathway was blocked [55]. In addition to Activin, KSR and insulin are present in MEF-CM, and these factors act as agonists of the PI3K-signaling pathway and thus could suppress definitive endoderm differentiation induced by Activin [55]. Furthermore, unknown factors contained in the MEF-CM might positively and strongly suppress the activity of Activin and the progression of differentiation into definitive endoderm.

Feasibility of Feeder-cell-free hiPSC Generation on PCM-DM with Non-conditioned Medium

In this study, we used MEF-CM in the initial phase of hiPSC generation, i.e., until the second passage, and StemPro medium thereafter. In the preliminary phase of this study, we tried using StemPro medium from the beginning of hiPSC generation, but we failed to generate hiPSCs, most likely owing to the limited proliferation of DMCs in StemPro medium. On the other hand, our analysis of the reprogramming efficiency of six different DMC lines under seven different culture conditions also showed that feeder-cell-free hiPSC generation on PCM-DM is feasible with both MEF-CM and NC-hESC medium, with comparable efficiency as on other substrates, and that clones generated and propagated without MEF-CM could stably maintain the cellular properties of hiPSCs. These findings suggest that MEF-CM is dispensable for generating hiPSCs on PCM-DM, and that various types of culture medium may be effective for generating hiPSCs on PCM-DM.

Although the most hESC-like colonies appeared on Matrigel with MEF-CM, both Matrigel and MEF-CM contain xenobiotic components, and thus may not be suitable for future clinical applications. Previous reports showed that hiPSCs can be

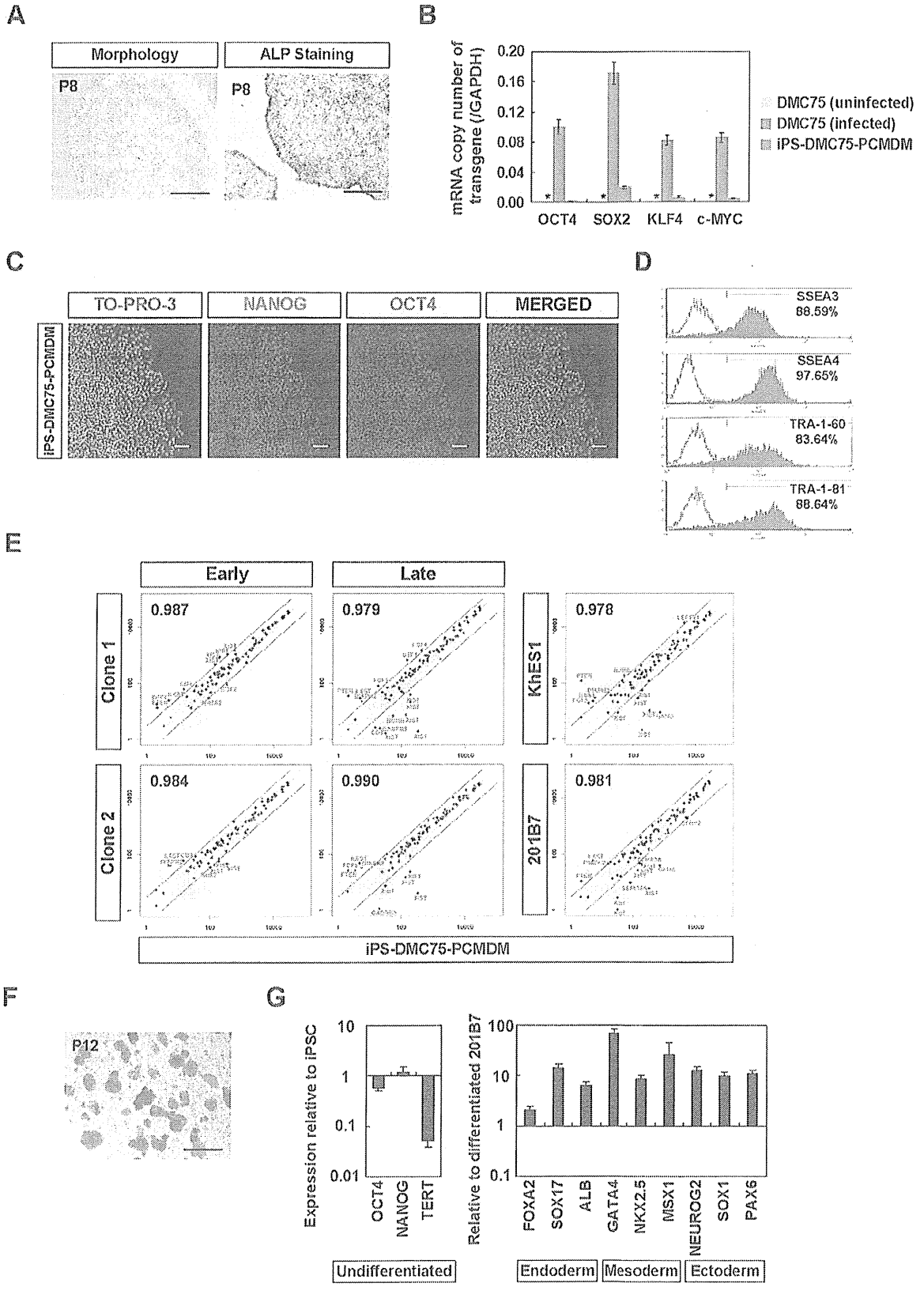
A
Morphology
ALP Staining
P8
P8
B
mRNA copy number of transgene (/GAPDH)
0.20
0.16
0.12
0.08
0.04
0.00
OCT4
SOX2
KLF4
c-MYC
DMC75 (uninfected)
DMC75 (infected)
iPS-DMC75-PCMDM
C
TO-PRO-3
NANOG
OCT4
MERGED
iPS-DMC75-PCMDM
D
SSEA3
88.59%
SSEA4
97.65%
TRA-1-60
83.64%
TRA-1-81
88.64%
E
Early
Late
Clone 1
0.987
0.979
KhES1
0.978
Clone 2
0.984
0.990
201B7
0.981
iPS-DMC75-PCMDM
F
P12
G
Expression relative to iPSC
10
1
0.1
0.01
OCT4
NANOG
TERT
Undifferentiated
Relative to differentiated 201B7
100
10
1
0.1
FOXA2
SOX17
ALB
GATA4
NKX2.5
MSX1
NEUROG2
SOX1
PAX6
Endoderm
Mesoderm
Ectoderm

Figure 9. Generation of hiPSCs from DMCs with non-conditioned hESC medium on PCM-DM. A) Morphology and Alkaline phosphatase (ALP) staining of iPS-DMC75-PCMDM. P, passage number. Scale bar = 500 μm. B). Quantitative RT-PCR analysis for the mRNA copy number of four transgenes (OCT4, SOX2, KLF4, c-MYC). All the transgenes were silenced in iPS-DMC75-PCMDM. Data are presented as the mean ± SD. *: not detected. C) Immunocytochemistry for NANOG (red) and OCT4 (green) expression in iPS-DMC75-PCMDM. Scale bar = 200 μm. D) Flow cytometry analysis for hESC-specific surface antigens (SSEA-3, SSEA-4, TRA-1-60, and TRA-1-81) at passage 11. E) Global gene expression analysis of iPS-DMC75-PCMDM (passage 12), early and late passages of clones 1 and 2, KhES1, and 201B7. Scatter plots and Pearson's coefficient are shown. The diagonal lines indicate 3-fold changes in gene expression levels. Plus ("+") symbols indicate stem-cell marker genes suggested by the International Stem Cell Initiative [31], and such genes outside the 3-fold change lines are shown in red text. Clone 1, iPS-DMC72-PCMDM01; Clone 2, iPS-DMC72-PCMDM02. F) Embryoid bodies (EBs) on day 8 derived from iPS-DMC75-PCMDM (passage 12). Scale bar = 500 μm. G) Quantitative RT-PCR analysis. Left, Expression levels of genes for the undifferentiated state in EBs relative to hiPSCs before differentiation. Right, Expression levels of lineage-specific genes in EBs relative to differentiated 201B7. Data are presented as the mean ± SD.
doi:10.1371/journal.pone.0055226.g009

generated from fibroblasts on gelatin-coated plates with NC-hESC medium [27] and that DMCs, like fibroblasts, have some maintenance activity for hESC/hiPSCs [23]. However, no hiPSC colonies were generated from DMCs on gelatin with NC-hESC medium (Fig. 8, Supplemental Table S5). This finding may indicate that the properties of DMCs acting as an auto-feeder on gelatin may be insufficient to generate hiPSCs in non-conditioned medium, and that feeder-cell-free generation on gelatin with non-conditioned medium might require modifications to generate different cell types. Our comparison of feeder-cell-free culture systems showed that culturing on PCM-DM is convenient, stable, and compatible with both MEF-CM and non-conditioned medium.

Taken together, our present results suggest that the combination of PCM-DM and StemPro medium might be slightly worse at maintaining hESCs/hiPSCs in an undifferentiated condition than the combination of PCM-DM and MEF-CM. Nevertheless, the pluripotency of the hiPSC-PCMDM was retained for over 20 passages, and the feeder-cell-free culture of hiPSCs using PCM-DM is practical and useful. Further improvements to the culture medium should increase the stability of the feeder-free-generated and cultured hiPSCs, and should be a topic of future studies.

PCM-DM may be a Useful Human-derived Matrix for Regenerative Medicine

Extra-embryonic tissues such as the umbilical cord and placenta have been suggested as attractive sources for human cells to be used in regenerative medicine. In this study, we used DMCs isolated from the decidua membrane, which is the maternal potion of the placenta [26]. DMCs exhibit a typical fibroblast-like morphology and have a high proliferative potential for over 30 population doublings, which is better than that of BM-MSCs [26]. They strongly express the mesenchymal cell marker vimentin, but not cytokeratin 19 or HLA-G, and FCM analysis showed that their expression pattern of cell-surface antigens closely resembles that of BM-MSCs [26]. In vitro, DMCs show good differentiation into chondrocytes and moderate differentiation into adipocytes, but little evidence of osteogenesis, compared with BM-MSCs [26]. These findings indicate that DMCs are mesenchymal cells of purely maternal origin, and that they are unique cells with MSC-like properties but differ from BM-MSCs. The greater proliferative ability of DMCs means that their cultivation might require less maintenance, and their derivation from the maternal portion of human fetal adnexal tissues, which are otherwise discarded, would resolve many ethical concerns associated with the use of embryonic cells. Moreover, the high success rate of DMC isolation from tissues stored more than 24 hours indicates that it might be feasible to develop a system for collecting or banking fetal adnexal tissues from multiple or even remote hospitals [26]. These properties of DMCs identify them as easily accessible human source for clinical uses. Our findings indicate that the generation of hiPSCs on PCM-DM, which has several advantages for clinical use, provides an opportunity to establish hiPSCs for clinical applications.

Conclusion

We generated hiPSCs that were stably maintained with respect to their self-renewal, pluripotency, and genome integrity over long-term culture on PCM-DM. Our findings indicate that PCM-DM can maintain and support the generation of hiPSCs. We suggest that PCM-DM is a practical and easily accessible, human-derived substrate that can be used, not just for the stable maintenance of hiPSCs, but also for their generation.

Supporting Information

Figure S1 Generation of hiPSCs from DMCs on PCM-DM. A) Morphology and Alkaline phosphatase (ALP) staining of iPS-DMC71-PCMDM and iPS-DMC92-PCMDM. P, passage number. Scale bar = 500 μm. B) Quantitative RT-PCR analysis for the mRNA copy number of four transgenes (OCT4, SOX2, KLF4, c-MYC). All the transgenes were silenced in the two hiPSC-PCMDM clones. Data are presented as the mean ± SD. *: not detected. B) Quantitative RT-PCR analysis for hESC marker gene (OCT4, SOX2, KLF4, c-MYC, NANOG) expression compared with hESCs (clone KhES1). Data are presented as the mean ± SD. C) Immunocytochemistry for NANOG (red) and OCT4 (green) expression in two hiPSC-PCMDM clones. Scale bar = 200 μm.
(TIF)

Table S1 Primers for quantitative RT-PCR.
(DOC)

Table S2 Primers for detecting the OCT4 and NANOG promoter.
(DOC)

Table S3 Results of short tandem repeat PCR (STR-PCR).
(DOC)

Table S4 Probe Set in Affymetrix Human Genome U133 Plus 2.0 Array for characterization of undifferentiated stem cells.
(DOC)

Table S5 Reprogramming efficiencies.
(DOC)

Acknowledgments

We thank Dr. Chiaki Ban (Department of Obstetrics and Gynecology Osaka National Hospital) and Ms. Chika Teramoto (Osaka National Hospital) for support in collecting the human placental tissues. We also thank Mr. Kenji Kawai and Ms. Miyuki Kuronuma (Central Institute for Experimental Animals) for support in Teratoma formation assay.

Author Contributions

Financial support: YK. Conceived and designed the experiments: HF YS YK. Performed the experiments: HF TS DK AY HS MN. Analyzed the data: HF TS AY HS MN MY MO YS YK. Wrote the paper: HF TS HS MN YS YK.

References

1. Takahashi K, Tanabe K, Ohnuki M, Narita M, Ichisaka T, et al. (2007) Induction of pluripotent stem cells from adult human fibroblasts by defined factors. Cell 131: 861–872.
2. Yu J, Vodyanik MA, Smuga-Otto K, Antosiewicz-Bourget J, Frane JL, et al. (2007) Induced pluripotent stem cell lines derived from human somatic cells. Science 318: 1917–1920.
3. Thomson JA, Itskovitz-Eldor J, Shapiro SS, Waknitz MA, Swiergiel JJ, et al. (1998) Embryonic stem cell lines derived from human blastocysts. Science 282: 1145–1147.
4. Reubinoff BE, Pera MF, Fong CY, Trounson A, Bongso A (2000) Embryonic stem cell lines from human blastocysts: somatic differentiation in vitro. Nat Biotechnol 18: 399–404.
5. Pan C, Hicks A, Guan X, Chen H, Bishop CE (2010) SNL fibroblast feeder layers support derivation and maintenance of human induced pluripotent stem cells. J Genet Genomics 37: 241–248.
6. Xu C, Inokuma MS, Denham J, Golds K, Kundu P, et al. (2001) Feeder-free growth of undifferentiated human embryonic stem cells. Nat Biotechnol 19: 971–974.
7. Rosler ES, Fisk GJ, Ares X, Irving J, Miura T, et al. (2004) Long-term culture of human embryonic stem cells in feeder-free conditions. Dev Dyn 229: 259–274.
8. Sun N, Panetta NJ, Gupta DM, Wilson KD, Lee A, et al. (2009) Feeder-free derivation of induced pluripotent stem cells from adult human adipose stem cells. Proc Natl Acad Sci U S A 106: 15720–15725.
9. Navarro-Alvarez N, Soto-Gutierrez A, Yuasa T, Yamatsuji T, Shirakawa Y, et al. (2008) Long-term culture of Japanese human embryonic stem cells in feeder-free conditions. Cell Transplant 17: 27–33.
10. Hayashi Y, Chan T, Warashina M, Fukuda M, Ariizumi T, et al. (2010) Reduction of N-glycolylneuraminic acid in human induced pluripotent stem cells generated or cultured under feeder- and serum-free defined conditions. PLoS One 5: e14099.
11. Lu J, Hou R, Booth CJ, Yang SH, Snyder M (2006) Defined culture conditions of human embryonic stem cells. Proc Natl Acad Sci U S A 103: 5688–5693.
12. Amit M, Shariki C, Margulets V, Itskovitz-Eldor J (2004) Feeder layer- and serum-free culture of human embryonic stem cells. Biol Reprod 70: 837–845.
13. Kitajima H, Niwa H (2010) Clonal expansion of human pluripotent stem cells on gelatin-coated surface. Biochem Biophys Res Commun 396: 933–938.
14. Rodin S, Domogatskaya A, Strom S, Hansson EM, Chien KR, et al. (2010) Long-term self-renewal of human pluripotent stem cells on human recombinant laminin-511. Nat Biotechnol 28: 611–615.
15. Miyazaki T, Futaki S, Hasegawa K, Kawasaki M, Sanzen N, et al. (2008) Recombinant human laminin isoforms can support the undifferentiated growth of human embryonic stem cells. Biochem Biophys Res Commun 375: 27–32.
16. Martin MJ, Muotri A, Gage F, Varki A (2005) Human embryonic stem cells express an immunogenic nonhuman sialic acid. Nat Med 11: 228–232.
17. Klimanskaya I, Rosenthal N, Lanza R (2008) Derive and conquer: sourcing and differentiating stem cells for therapeutic applications. Nat Rev Drug Discov 7: 131–142.
18. Hovatta O, Mikkola M, Gertow K, Stromberg AM, Inzunza J, et al. (2003) A culture system using human foreskin fibroblasts as feeder cells allows production of human embryonic stem cells. Hum Reprod 18: 1404–1409.
19. Cheng L, Hammond H, Ye Z, Zhan X, Dravid G (2003) Human adult marrow cells support prolonged expansion of human embryonic stem cells in culture. Stem Cells 21: 131–142.
20. Richards M, Tan S, Fong CY, Biswas A, Chan WK, et al. (2003) Comparative evaluation of various human feeders for prolonged undifferentiated growth of human embryonic stem cells. Stem Cells 21: 546–556.
21. Amit M, Margulets V, Segev H, Shariki K, Laevsky I, et al. (2003) Human feeder layers for human embryonic stem cells. Biol Reprod 68: 2150–2156.
22. Anchan RM, Quaas P, Gerami-Naini B, Bartake H, Griffin A, et al. (2011) Amniocytes can serve a dual function as a source of iPS cells and feeder layers. Hum Mol Genet 20: 962–974.
23. Nagase T, Ueno M, Matsumura M, Muguruma K, Ohgushi M, et al. (2009) Pericellular matrix of decidua-derived mesenchymal cells: a potent human-derived substrate for the maintenance culture of human ES cells. Dev Dyn 238: 1118–1130.
24. Suemori H, Yasuchika K, Hasegawa K, Fujioka T, Tsuneyoshi N, et al. (2006) Efficient establishment of human embryonic stem cell lines and long-term maintenance with stable karyotype by enzymatic bulk passage. Biochem Biophys Res Commun 345: 926–932.
25. Amit M, Carpenter MK, Inokuma MS, Chiu CP, Harris CP, et al. (2000) Clonally derived human embryonic stem cell lines maintain pluripotency and proliferative potential for prolonged periods of culture. Dev Biol 227: 271–278.
26. Kanematsu D, Shofuda T, Yamamoto A, Ban C, Ueda T, et al. (2011) Isolation and cellular properties of mesenchymal cells derived from the decidua of human term placenta. Differentiation 82: 77–88.
27. Takahashi K, Narita M, Yokura M, Ichisaka T, Yamanaka S (2009) Human induced pluripotent stem cells on autologous feeders. PLoS One 4: e8067.
28. Livak KJ, Schmittgen TD (2001) Analysis of relative gene expression data using real-time quantitative PCR and the 2(-Delta Delta C(T)) Method. Methods 25: 402–408.
29. Edgar R, Domrachev M, Lash AE (2002) Gene Expression Omnibus: NCBI gene expression and hybridization array data repository. Nucleic Acids Res 30: 207–210.
30. Ito M, Hiramatsu H, Kobayashi K, Suzue K, Kawahata M, et al. (2002) NOD/SCID/gamma(c)(null) mouse: an excellent recipient mouse model for engraftment of human cells. Blood 100: 3175–3182.
31. Adewumi O, Aflatoonian B, Ahrlund-Richter L, Amit M, Andrews PW, et al. (2007) Characterization of human embryonic stem cell lines by the International Stem Cell Initiative. Nat Biotechnol 25: 803–816.
32. Yap LY, Li J, Phang IY, Ong LT, Ow JZ, et al. (2011) Defining a threshold surface density of vitronectin for the stable expansion of human embryonic stem cells. Tissue Eng Part C Methods 17: 193–207.
33. Braam SR, Zeinstra L, Litjens S, Ward-van Oostwaard D, van den Brink S, et al. (2008) Recombinant vitronectin is a functionally defined substrate that supports human embryonic stem cell self-renewal via alphavbeta5 integrin. Stem Cells 26: 2257–2265.
34. Prowse AB, Doran MR, Cooper-White JJ, Chong F, Munro TP, et al. (2010) Long term culture of human embryonic stem cells on recombinant vitronectin in ascorbate free media. Biomaterials 31: 8281–8288.
35. Chen G, Gulbranson DR, Hou Z, Bolin JM, Ruotti V, et al. (2011) Chemically defined conditions for human iPSC derivation and culture. Nat Methods 8: 424–429.
36. Furue MK, Na J, Jackson JP, Okamoto T, Jones M, et al. (2008) Heparin promotes the growth of human embryonic stem cells in a defined serum-free medium. Proc Natl Acad Sci U S A 105: 13409–13414.
37. Nagaoka M, Si-Tayeb K, Akaike T, Duncan SA (2010) Culture of human pluripotent stem cells using completely defined conditions on a recombinant E-cadherin substratum. BMC Dev Biol 10: 60.
38. Stojkovic P, Lako M, Przyborski S, Stewart R, Armstrong L, et al. (2005) Human-serum matrix supports undifferentiated growth of human embryonic stem cells. Stem Cells 23: 895–902.
39. Escobedo-Lucea C, Stojkovic M (2010) Growth of human embryonic stem cells using derivates of human fibroblasts. Methods Mol Biol 584: 55–69.
40. Meng G, Liu S, Li X, Krawetz R, Rancourt DE (2010) Extracellular matrix isolated from foreskin fibroblasts supports long-term xeno-free human embryonic stem cell culture. Stem Cells Dev 19: 547–556.
41. Fu X, Toh WS, Liu H, Lu K, Li M, et al. (2011) Establishment of Clinically Compliant Human Embryonic Stem Cells in an Autologous Feeder-Free System. Tissue Eng Part C Methods 927–937.
42. Nishimoto M, Fukushima A, Okuda A, Muramatsu M (1999) The gene for the embryonic stem cell coactivator UTF1 carries a regulatory element which selectively interacts with a complex composed of Oct-3/4 and Sox-2. Mol Cell Biol 19: 5453–5465.
43. Yuan H, Corbi N, Basilico C, Dailey L (1995) Developmental-specific activity of the FGF-4 enhancer requires the synergistic action of Sox2 and Oct-3. Genes Dev 9: 2635–2645.
44. Levine AJ, Brivanlou AH (2006) GDF3, a BMP inhibitor, regulates cell fate in stem cells and early embryos. Development 133: 209–216.
45. Levine AJ, Brivanlou AH (2006) GDF3 at the crossroads of TGF-beta signaling. Cell Cycle 5: 1069–1073.
46. Caricasole AA, van Schaik RH, Zeinstra LM, Wierikx CD, van Gurp RJ, et al. (1998) Human growth-differentiation factor 3 (hGDF3): developmental regulation in human teratocarcinoma cell lines and expression in primary testicular germ cell tumours. Oncogene 16: 95–103.
47. Beattie GM, Lopez AD, Bucay N, Hinton A, Firpo MT, et al. (2005) Activin A maintains pluripotency of human embryonic stem cells in the absence of feeder layers. Stem Cells 23: 489–495.
48. Shofuda T, Kanematsu D, Fukusumi H, Yamamoto A, Bamba Y, et al. (2013) Human Decidua-Derived Mesenchymal Cells are a Promising Source for the Generation and Banking of Human Induced Pluripotent Stem Cells. Cell Med: in press.
49. Tchieu J, Kuoy E, Chin MH, Trinh H, Patterson M, et al. (2010) Female human iPSCs retain an inactive X chromosome. Cell Stem Cell 7: 329–342.
50. Silva SS, Rowntree RK, Mekhoubad S, Lee JT (2008) X-chromosome inactivation and epigenetic fluidity in human embryonic stem cells. Proc Natl Acad Sci U S A 105: 4820–4825.
51. Lengner CJ, Gimelbrant AA, Erwin JA, Cheng AW, Guenther MG, et al. (2010) Derivation of pre-X inactivation human embryonic stem cells under physiological oxygen concentrations. Cell 141: 872–883.

52. Shen Y, Matsuno Y, Fouse SD, Rao N, Root S, et al. (2008) X-inactivation in female human embryonic stem cells is in a nonrandom pattern and prone to epigenetic alterations. Proc Natl Acad Sci U S A 105: 4709–4714.
53. Hall LL, Byron M, Butler J, Becker KA, Nelson A, et al. (2008) X-inactivation reveals epigenetic anomalies in most hESC but identifies sublines that initiate as expected. J Cell Physiol 216: 445–452.
54. Vallier L, Touboul T, Chng Z, Brimpari M, Hannan N, et al. (2009) Early cell fate decisions of human embryonic stem cells and mouse epiblast stem cells are controlled by the same signalling pathways. PLoS One 4: e6082.
55. McLean AB, D'Amour KA, Jones KL, Krishnamoorthy M, Kulik MJ, et al. (2007) Activin a efficiently specifies definitive endoderm from human embryonic stem cells only when phosphatidylinositol 3-kinase signaling is suppressed. Stem Cells 25: 29–38.
56. Wang L, Schulz TC, Sherrer ES, Dauphin DS, Shin S, et al. (2007) Self-renewal of human embryonic stem cells requires insulin-like growth factor-1 receptor and ERBB2 receptor signaling. Blood 110: 4111–4119.
57. D'Amour KA, Agulnick AD, Eliazer S, Kelly OG, Kroon E, et al. (2005) Efficient differentiation of human embryonic stem cells to definitive endoderm. Nat Biotechnol 23: 1534–1541.

http://informahealthcare.com/xen
ISSN: 0049-8254 (print), 1366-5928 (electronic)

Xenobiotica

Xenobiotica, 2014; 44(2): 146–153
© 2014 Informa UK Ltd. DOI: 10.3109/00498254.2013.836257

informa
healthcare

RESEARCH ARTICLE

The human hepatic cell line HepaRG as a possible cell source for the generation of humanized liver TK-NOG mice

Yuichiro Higuchi[1], Kenji Kawai[1], Hiroshi Yamazaki[2], Masato Nakamura[3], Françoise Bree[4], Christiane Guguen-Guillouzo[5], and Hiroshi Suemizu[1]

[1]*Central Institute for Experimental Animals, Kawasaki, Kanagawa, Japan,* [2]*Laboratory of Drug Metabolism and Pharmacokinetics, Showa Pharmaceutical University, Machida, Tokyo, Japan,* [3]*Tokai University School of Medicine, Isehara, Kanagawa, Japan,* [4]*XENOBLIS, Saint Grégoire, France, and* [5]*Biopredic International, Rennes, France*

Xenobiotica Downloaded from informahealthcare.com by 218.33.133.54 on 01/24/14
For personal use only.

Abstract

1. Humanized-liver mice, in which the liver has been repopulated with human hepatocytes, have been used to study aspects of human liver physiology such as drug metabolism, toxicology and hepatitis infection. However, the procurement of human hepatocytes is a major problem in producing humanized-liver mice because of the finite nature of the patient-derived resource.
2. In order to overcome this limitation, the human hepatic cell line HepaRG™ were evaluated as promising donor cells for liver reconstitution in the TK-NOG mouse model.
3. We demonstrate that, *in vivo*, transplanted confluent culture or differentiated HepaRG® cells proliferated and differentiated toward both hepatocyte-like and biliary-like cells within the recipient liver. In contrast, proliferative HepaRG® cells could engraft TK-NOG mouse liver but could differentiate only toward biliary-like cells. The differentiation to hepatocyte-like cells was characterized by the detection of human albumin in the recipient mouse serum and was confirmed by immunohistochemical staining for human leukocyte antigen, human albumin, cytochrome P450 3A4, and multidrug resistance-associated protein 2. Biliary-like cells were characterized by positive staining for cytokeratin-19.
4. These results indicated that the differentiated HepaRG® cells are a possible cell source for generating humanized-liver mice, which are a useful model for *in vivo* studies of liver physiology.

Keywords

HepaRG, human hepatocytes, humanized-liver mice, TK-NOG mouse

History

Received 21 June 2013
Revised 15 August 2013
Accepted 15 August 2013
Published online 25 September 2013

Introduction

The liver performs many complex functions, including carbohydrate, urea and lipid metabolism, storage of essential nutrients, production of plasma proteins and secretion of bile acids, metabolism of drugs and other compounds and excretion of the metabolites into bile canaliculi. Although primary cultured hepatocytes are the standard model for xenobiotic metabolism and toxicity studies, an *in vitro* culture method that maintains the *in vivo* functions of the hepatocytes has not been established (Nibourg et al., 2012). To overcome this issue, we and other groups have developed humanized-liver mice in which the liver is reconstituted with human liver cells for studying *in vivo* drug metabolism and liver regeneration (Azuma et al., 2007; Dandri et al., 2001; Hasegawa et al., 2011; Mercer et al., 2001). The reconstituted livers also express enzymes found in human hepatocytes, and they can generate human-specific metabolites of test substrates, including steroids. One of the problems in generating humanized-liver mice is the cell source for liver reconstitution. Commercially available cryopreserved human hepatocytes are the easiest to use for generating humanized-liver mice at present; however, it is well known that individual differences not only affect the success rate of generating chimeric mice but also influence the drug-metabolizing properties of the humanized livers. As primary human hepatocytes never successfully proliferate *in vitro*, it is difficult to stably generate humanized-liver mice with finite hepatocytes.

Novel cell sources that can proliferate *in vitro* and reconstitute the liver *in vivo* are needed to achieve steady generation of humanized-liver mice. In this study, we focused on HepaRG® cells as a cell source for generating humanized-liver mice. HepaRG™ is an immortalized cell line that was isolated from a hepatic-differentiated grade 1 Edmonson hepatocholangiocarcinoma (Gripon et al., 2002). Previous studies have demonstrated that bipotent progenitor HepaRG™ cells that have the ability to differentiate into both hepatocyte-like and biliary-like epithelial phenotypes *in vitro* (Cerec et al., 2007). Because fully differentiated HepaRG™ cells express physiologic functions similar to primary cultured human hepatocytes, they are regarded as an *in vitro* model

Address for correspondence: Hiroshi Suemizu, PhD, Central Institute for Experimental Animals, 3-25-12 Tonomachi, Kawasaki-ku, Kawasaki, Kanagawa 210-0821, Japan. Tel: +81-44-201-8530. Fax: +81-44-201-8541/+81-44-201-8511. E-mail: suemizu@ciea.or.jp

RIGHTSLINK

DOI: 10.3109/00498254.2013.836257

of drug metabolism (Guillouzo et al., 2007; Kanebratt & Andersson, 2008). A few studies have reported the successful engraftment of HepaRG® cells into the mouse liver (Cerec et al., 2007; Jiang et al., 2010) and have described the *in vivo* expression of human serum albumin from the transplanted HepaRG® cells. However, the engraftment of HepaRG® cells was confirmed by immunohistochemical staining with the mature hepatocyte marker albumin, and the expression of drug-metabolizing enzymes *in vivo* has not been investigated. Thus, it remains unclear whether HepaRG® cells engrafted into the mouse liver preserve their capacity to undergo complete hepatocyte maturation *in vivo*.

Recently, we developed a novel humanized model with inducible liver injury platform consisting of the targeted expression of the herpes simplex virus type 1 thymidine kinase (HSV-TK) in the liver of severely immunodeficient NOG mice (TK-NOG) (Hasegawa et al., 2011). A brief exposure to a non-toxic dose of ganciclovir (GCV) causes mouse liver cells expressing the transgene to be ablated. Then, the transplanted human hepatocytes are stably maintained within the liver of TK-NOG mice in the absence any exogenous drug or immunosuppressive treatments. However, the procurement of human hepatocytes is a major problem in producing humanized-liver mice because of the finite nature of the patient-derived resource. Therefore, we evaluate HepaRG® cells as promising donor cells for liver reconstitution in the TK-NOG mouse model to over come this problem.

Materials and methods

HepaRG® cells

In accordance with the manufacturer's protocol, HepaRG® cells were maintained in HepaRG® maintenance medium (Biopredic International, Rennes, France). For differentiation, HepaRG® cells were seeded onto six-well plates at a density of 2×10^4 cells/cm^2. Cells were cultured in maintenance medium until the seventh day after plating, when the medium was replaced with HepaRG® differentiation medium containing 1.7% dimethyl sulfoxide (DMSO) (Biopredic International, Rennes, France). Both the maintenance medium and the differentiation medium were changed every 2 days.

Real-time quantitative reverse transcription polymerase chain reaction for expression of drug metabolism-related genes

Total RNA was obtained from HepaRG® cells for each day of differentiation using the RNeasy Mini Kit (Qiagen K.K., Tokyo, Japan). Real-time quantitative reverse transcription polymerase chain reaction (RT-PCR) was performed using the High Capacity cDNA Reverse Transcription kit (Life Technologies Corporation, Grand Island, NY). The TaqMan Gene Expression Master Mix and TaqMan Gene Expression Assays (Life Technologies Corporation, Grand Island, NY) were used for RT-PCR, and amplification was then carried out using an ABI Prism 7000 Sequence Detection System (Life Technologies Corporation, Grand Island, NY). The amount of cDNA was normalized to the expression level of glyceraldehyde 3-phosphate dehydrogenase (GAPDH). The TaqMan Assay number is listed in Supplementary Table 1.

Induction of liver damage

All mouse studies were conducted in strict accordance with the Guide for the Care and Use of Laboratory Animals of the Central Institute for Experimental Animals, and the experimental protocols were approved by the Animal Care Committee of CIEA (Permit Number: 11029A). All surgeries were performed under isoflurane anesthesia, and all efforts were made to minimize suffering. The TK-NOG strain (Hasegawa et al., 2011) was maintained by breeding female Tg TK-NOG mice with male non-Tg TK-NOG littermates, and the transgenic offspring were selected by genotyping with the following TaqMan probe set: forward primer (TaqMan-TKF), 5′-CCATGCACGTCTTTATCCTGG-3′; reverse primer (TaqMan-TKR), 5′-TAAGTTGCAGCAGGG CGTC-3′; and TaqMan probe (TK-FAM), 5′-FAM-AATCGC CCGCCGGCTGC-MGB-3′. Adult 8–10-week-old male TK-NOG mice were injected intraperitoneally with GCV sodium (6 mg/kg, Denosine-IV; Mitsubishi Tanabe Pharma Corporation, Osaka, Japan) every other day to ablate mouse liver cells expressing HSV-TK transgene. One week after GCV treatment, the degree of liver damage was examined by determining serum aspartate aminotransferase (AST) and alanine aminotransferase (ALT) values using an automated clinical chemistry analyzer FUJI DRI-CHEM 7000 (Fuji Photo Film Co. Ltd. Tokyo, Japan).

Transplantation

On Days 1, 7, 21 or 35 after plating, differentiated HepaRG® cells were dissociated by 0.25% trypsin–EDTA and transplanted into TK-NOG mouse.

Cryopreserved human hepatocytes (HEP187170; 26 years, female; Biopredic International, Rennes, France) were used as a positive control for transplantation.

A total of 1×10^6 cells in 40 µl of Hank's Balanced Salt Solution (HBSS, Life Technologies Corporation, Grand Island, NY) were intrasplenically injected using a Hamilton syringe with a 26 gauge needle, as previously described (Suemizu et al., 2008). The successful engraftment of the HepaRG® cells and the HEP187170 hepatocytes was evaluated by measuring increases in the mouse blood level of human albumin (hAlb) with a Human Albumin ELISA Quantitation Kit (Bethyl Laboratories, Montgomery, TX), according to the manufacturer's protocol. The extent of reconstitution with human hepatocytes was estimated as a function of the hAlb concentration, which was shown to correlate with the extent of human liver replacement (Hasegawa et al., 2011). Twelve weeks after transplantation, recipient livers were recovered and fixed with 10 nM Mildform formaldehyde solution (Wako Pure Chemical Industries, Ltd., Osaka, Japan). To evaluate the growth potential of the HepaRG® cell lines *in vivo*, TK-NOG mice received a subcutaneous (s.c.) injection of 1×10^6 HepaRG® cells suspended in 0.1 ml of HBSS and 0.1 ml of Matrigel (BD Biosciences, Bedford, MA). The human hepatocellular carcinoma cell line HepG2 (obtained from the American Type Culture Collection; Manassas, VA) that has the ability to form subcutaneous xenografts was used as positive control. A total of 1×10^4 HepG2 cells were suspended in 0.1 ml of HBSS:Matrigel in a 1:1 solution and injected s.c. Apparent

Xenobiotica Downloaded from informahealthcare.com by 218.33.133.54 on 01/24/14
For personal use only.

RIGHTSLINK

tumors were measured biweekly. The tumor volume (TV) was calculated using the formula $TV = \times A \times B^2$ [A: length (mm); B: width (mm)].

Histology and immunohistochemistry

Formalin-fixed tissues were embedded in paraffin and then sliced and analyzed by either hematoxylin–eosin staining (H&E) or immunohistochemistry. Some sections were autoclaved for 10 min in a target retrieval solution (0.1 M citrate buffer, pH 6.0; 1 mM EDTA, pH 9.0) and then placed at room temperature for 20 min. The following antibodies were used for immunohistochemical analysis: monoclonal mouse anti-human leukocyte antigen (HLA) Class I (A, B and C) (clone EMR8-5; Hokudo, Sapporo, Japan), polyclonal goat anti-human albumin (Bethyl Laboratories, Montgomery, TX), anti-cytokeratin-19 (CK-19, Novocastra Laboratories Ltd., Newcastle, UK), polyclonal rabbit anti-cytochrome P450 3A4 (CYP3A4) (Abcam Inc., Cambridge, MA) and anti-human multidrug resistance-associated protein 2 (MRP2) (clone M2 III-6; Merck Millipore, Billerica, MA). The antibodies for mouse, goat and rabbit immunoglobulins were visualized using amino acid polymer/peroxidase complex-labeled antibodies [Histofine Simple Stain Mouse MAX PO (M, G and R); Nichirei Bioscience, Tokyo, Japan] and a diaminobenzidine (DAB; Dojindo Laboratories, Kumamoto, Japan) substrate (0.2 mg/mL 3,3′-diaminobenzidine tetrahydrochloride, 0.05 M Tris–HCl, pH 7.6, and 0.005% H_2O_2). Sections were counterstained with hematoxylin. A periodic acid-Schiff (PAS) staining kit (Muto Pure Chemicals, Tokyo, Japan) was used for visualizing glycogen. The images were captured under an upright microscope Axio Imager (Carl Zeiss, Thornwood, NY) equipped with AxioCam HRm and AxioCam MRc5 CCD cameras (Carl Zeiss). The HepaRG$^{®}$ cell colonies containing >20 HLA-positive cells on the cross-sections of three to five lobes of the TK-NOG mouse liver were counted. The areas (in centimeters) of the immunohistochemical sections were measured by using the Image Processing and Analysis in Java software (ImageJ version 1.46, http://imagej.nih.gov/ij/). Colony formation was evaluated as the number of colonies per area of observation (colonies/cm^2).

Results

HepaRG$^{®}$ cells reconstitute the TK-NOG mouse liver

According to the manufacturer's protocol, the HepaRG$^{®}$ cells were seeded at low confluency in six-well culture plates (2×10^4 cells/cm^2; Day 1) to induce transdifferentiation (Cerec et al., 2007). The cells reached 100% confluency within 1 week (Day 7), and the medium was then replaced with the differentiation medium, which contained 1.7% DMSO. The hepatocyte-like cells, which are similar to mono- or bi-nucleated human hepatocytes, appeared 21 days after seeding (Figure 1A). The gene expression of the following drug metabolism-related molecules, in the HepaRG$^{®}$ cell differentiation cultures, was analyzed on Days 1, 7, 21 and 35 by qPCR: 12 CYP450 and 2 phase II enzymes, 5 SLC

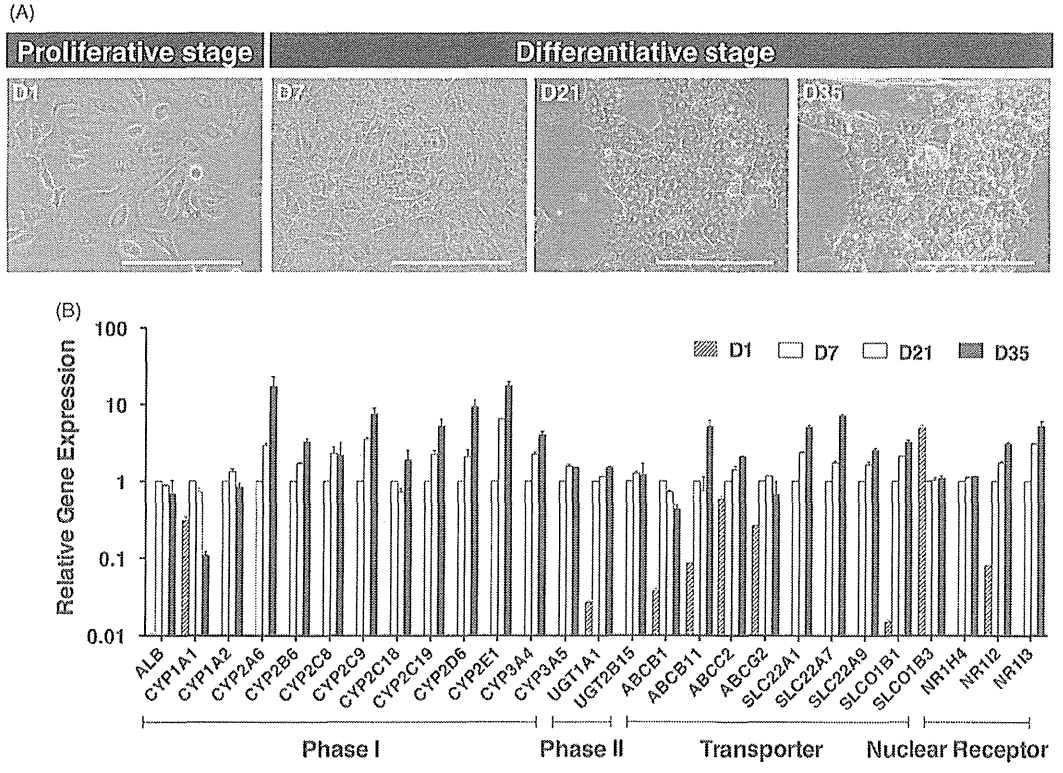

Figure 1. *In vitro* differentiation of HepaRG$^{®}$ cells. (A) Phase-contrast photographs of HepaRG$^{®}$ cells at the proliferative stage (D1: low-density culture), and the differentiative stage (D7: confluent culture; D21 and D35: differentiation culture with 1.7% DMSO). D1, 7, 21 and 35 in HepaRG$^{®}$ stage indicate the number of days after seeding. Bar = 100 μm. (B) The relative expression of 26 human drug metabolism-related mRNAs on D1, 7, 21 or 35 in the HepaRG$^{®}$ cells was assessed by qPCR. Each bar represents the average of two independent determinations, and the standard error is shown.

RIGHTSLINK

Xenobiotica Downloaded from informahealthcare.com by 218.33.133.54 on 01/24/14
For personal use only.

Table 1. Colony-forming ability of various differentiation stages of HepaRG™ cells in TK-NOG livers.

Experiment No.	HepaRG™ stage	Mouse ID No.	BW (g)	hAlb (μg/mL)	Area (cm^2)	Hepatocyte-like colony		Biliary-like colony	
						Number	Colonies/cm^2	Number	Colonies/cm^2
1	D35	2	15.2	ND	3.6	0	0	0	0
		3	24.0	ND	4.3	6	1.4	5	1.2
		4	26.5	ND	3.7	1	0.3	0	0
		5	25.7	ND	4.0	0	0	1	0.3
		8	27.0	ND	4.0	7	1.8	1	0.3
2	D1	2	28.6	ND	3.3	0	0	0	0
		3	28.0	ND	4.9	0	0	31	6.3
	D7	1	27.9	6.9	4.5	24	5.3	43	9.5
		5	28.9	ND	4.0	3	0.7	23	5.7
	D21	9	26.9	14.2	3.8	40	10.5	26	6.8
		14	26.5	ND	2.9	21	7.4	37	13.0
	D35	10	25.2	ND	2.8	2	0.7	1	0.4
		12	27.7	ND	3.0	4	1.3	4	1.3

D1, 7, 21 and 35 in HepaRG™ stage indicate the number of days after seeding. BW: body weight. The hAlb level of each animal is shown. ND: not detected by ELISA. Area: observed cross-sections were measured and indicated as centimeter square (cm^2). Colonies per centimeter square (colonies/cm^2): number of colonies per area of observation.

Xenobiotica Downloaded from informahealthcare.com by 218.33.133.54 on 01/24/14
For personal use only.

and 4 ABC transporters, and 3 nuclear hormone receptors (Figure 1B). As previously reported, the gene expression levels of the major drug metabolism enzymes and transporters were markedly increased in differentiative stage (>Day 7) compared to proliferative stage (Day 1) of HepaRG™ cells, except for SLCO1B3. We then intrasplenically transplanted fully differentiated HepaRG™ cells (Day 35) into five TK-NOG mice to investigate the functionality of the transplanted HepaRG™ cells *in vivo* (Table 1). Twelve weeks after transplantation, the engraftment of the HepaRG™ cells was demonstrated by human-specific marker staining: four-fifths of recipients showed the formation of HLA-positive cell colonies, suggesting that their livers had been repopulated with the transplanted human cells. The HLA-positive engrafted cell colonies were categorized by morphological differences into either hepatocyte-like cell colonies that were organized as polygonal cells with characteristic round nucleus or biliary-like cell colonies that were organized as ductal epithelial cells (Figure 2). Histological analysis of the recipient livers suggests that the HepaRG™ cells differentiated into mature hepatocyte or biliary cell lineages *in vivo*. To confirm this result, we performed immunohistochemical analysis for hepatocyte or biliary cell markers. Consistent with morphological characteristics, hepatocyte-like colonies were stained with the hepatocyte marker human albumin and were not stained with the biliary marker CK-19 (Figure 2, upper panel), whereas biliary-like colonies were found to be Alb-negative/CK-19-positive colonies (Figure 2, lower panel).

HepaRG™-derived hepatocyte-like cells have the characteristics of mature hepatocytes

We have demonstrated that fully differentiated HepaRG™ cells (Day 35) have the potential to transdifferentiate into both hepatocyte and biliary cells *in vivo* through bipotent progenitors in TK-NOG mice; however, the chimerism of the livers reconstituted with HepaRG™ cells was extremely low, and human albumin was undetectable in mouse plasma. HepaRG™ cells at various differentiation conditions (Day 1, 7, 21 and 35) were intrasplenically injected into TK-NOG mice to identify a suitable differentiation stage for optimal reconstitution of the mouse liver. Twelve weeks after transplantation, successful engraftment was determined using ELISA to detect the serum level of human albumin and was confirmed by histological analysis of TK-NOG mice livers. Human albumin was detected in two animals (2 out of 8) that had received 7-day (6.9 μg/ml) and 21-day (14.2 μg/ml) HepaRG™ cells (Table 1). The HepaRG-derived colonies, which were categorized by morphologic characteristics into hepatocyte-like and biliary-like, were counted according to the criteria described in the "Materials and methods" section (Table 1). Interestingly, undifferentiated (proliferative) HepaRG™ cells (Day 1) only differentiated into biliary-like cells *in vivo*; we failed to identify the differentiation into hepatocyte-like cells. In contrast, differentiated HepaRG™ cells corresponding to cultures at Days 7 and 21 days were successfully engrafted, and gave rise to both hepatocyte-like and biliary-like cells in TK-NOG mouse livers. However, the repopulation and expansion potentials were markedly decreased in the fully differentiated HepaRG™ cells (Day 35). Consistent with the hAlb ELISA result, an increased number of hepatocyte-like colonies was observed in the livers of recipient animals; this finding was confirmed by the production of detectable levels of human albumin (Table 1).

Next, the hepatocytic functionality of the differentiated HepaRG™ cells was evaluated by histochemistry and immunohistochemistry. We compared mature human hepatocyte characteristics, including glycogen accumulation and the expression of the CYP3A4 and MRP2 proteins, between hepatocyte-like colonies in mouse livers repopulated with differentiated HepaRG™ cells (day 21) and hepatocyte colonies in mouse livers repopulated with the HEP187170 hepatocytes, respectively. Successful engraftment of the HEP187170 hepatocytes was determined 12 weeks after transplantation by detecting the serum level of human albumin using ELISA. Human albumin was detected in all the HEP187170 hepatocytes transplanted animals (eight out of eight) with varied concentration (Table 2).

The human hepatocytes could be clearly distinguished from mouse hepatocytes by their pale cytoplasm in H&E

RIGHTSLINK

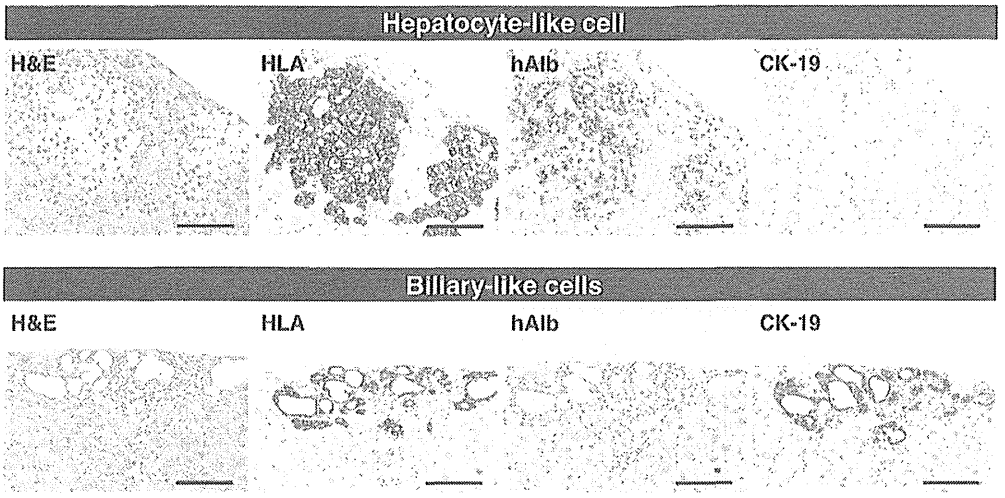

Figure 2. Reconstitution of human liver structures from differentiated HepaRG™ cells *in vivo*. Hepatocyte-like colonies (upper panel) and biliary-like colonies (lower panel) in a TK-NOG mouse liver that was transplanted with differentiation D35 HepaRG™ cells were subjected to immunohistochemical analysis. Serial liver sections were stained for H&E, HLA, hAlb and CK-19. Bar = 100 μm.

Table 2. Engraftment of cryopreserved human hepatocytes in TK-NOG livers.

Cryopreserved hepatocytes	Mouse ID No.	BW (g)	hAlb (μg/mL)	RI (%)
HEP187170	73	24.7	1459	20.9
	78	27.5	684	12.0
	79	27.9	1061	16.3
	712	21.0	2778	36.0
HEP187170	714	18.6	2818	36.4
	102	22.0	4803	59.1
	113	21.5	3355	42.6
	114	20.6	5115	62.7

The amount of hAlb and extent of human liver reconstitution in TK-NOG mice were measured 12 weeks after transplantation of cryopreserved human hepatocytes (HEP187170). BW: body weight. The extent of human liver reconstitution was estimated as a function of the hAlb concentration, which was shown to correlate with the extent of human liver reconstitution. RI: reconstitution index.

stained sections and by glycogen accumulation, which was restricted to the cytoplasm of the human hepatocytes in PAS-stained sections (Figure 3, lower panel); these findings are consistent with previous descriptions (Hasegawa et al., 2011). Hepatocyte-like cells exhibited H&E and PAS staining profiles similar to those of human hepatocytes (Figure 3, upper panel). Furthermore, the immunohistochemical analysis of hepatocyte-like cells revealed that the expression of a major drug-metabolizing enzyme in the liver, CYP3A4, and a major organic anion transporter in bile excretion in the liver, MRP2, expression level of which were also similar to those of humanized livers repopulated by the HEP187170 hepatocytes (Figure 3, upper and lower panel). These results imply that the hepatocyte-like cells that were differentiated *in vivo* could preserve similar drug-metabolizing activities to those of HepaRG™ cells that were differentiated *in vitro*.

Negligibly low tumorigenicity of HepaRG™ cells

If tumorigenic abilities remained in the HepaRG™ cells, the humanized liver, which was repopulated with the human hepatocyte-like HepaRG™ cells, will likely become cancerous. Therefore, the tumorigenicity of the HepaRG™ cells was assessed using severely immunocompromised NOG mice. Day 1 and Day 35 HepaRG™ cells (1×10^6 cells) as well as hepatocellular carcinoma HepG2 cells (1×10^4 cells; positive control) were subcutaneously transplanted into NOG mice. Subcutaneously formed xenografts were observed 3 weeks after transplantation. HepG2 cells grew rapidly forming tumors of 1000 mm^3 within 7 weeks, whereas both the Day 1 (proliferative stage) and Day 35 (fully differentiated stage) HepaRG™ cell grafts did not increase in size throughout the observation period (12 and 7 weeks, respectively), even though the HepaRG™ cells were introduced at a concentration 100 times greater than the control HepG2 cells (Figure 4A). Twelve weeks after transplantation, the HepaRG™ cell grafts (Day 1) were analyzed by immunohistochemical staining (Figure 4B). The few HLA-positive surviving cells were observed in a gelatinous matrix. These remaining cells did not express albumin but expressed the biliary-lineage marker CK-19. From these results, it was hypothesized that the negligibly low tumorigenicity of the HepaRG™ cells would not affect the generation of humanized-liver mice.

Discussion

In this study, we report that the human hepatic cell line HepaRG™ is a promising cell source for the steady generation of humanized-liver mice. Using differentiated HepaRG™ cells, we have demonstrated *in vivo* the transdifferentiation of both hepatocyte-like and biliary-like cell populations into hepatocytic and biliary lineages through a common hepatic progenitor that actively proliferates. Previous studies have described *in vitro* differentiation from proliferative HepaRG™ cells to mature hepatocyte-like cells that express liver-specific marker proteins or mRNAs, such as albumin and CYP3A4 (Cerec et al., 2007; Gripon et al., 2002). We also confirmed that the CYP mRNAs were undetectable in the proliferative stage in HepaRG™ cells, whereas at the differentiation stage,

RIGHTSLINK

Xenobiotica Downloaded from informahealthcare.com by 218.33.133.54 on 01/24/14
For personal use only.

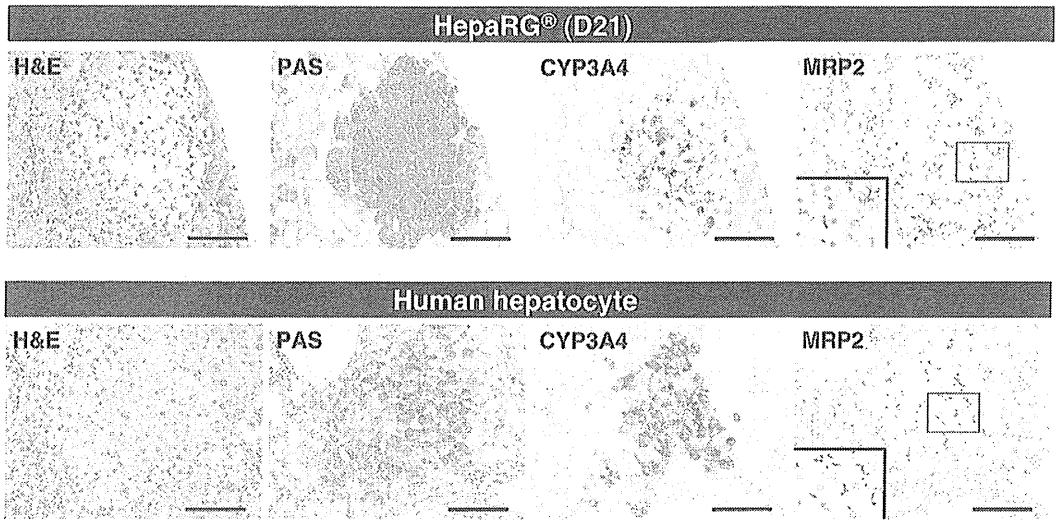

Figure 3. Expression of functional liver markers in reconstituted livers from TK-NOG mice. Hepatocyte-like colonies in a TK-NOG mouse liver that was transplanted with differentiation D21 HepaRG® cells (upper panel) and human hepatocyte colonies in a TK-NOG mouse liver that was transplanted with cryopreserved human hepatocytes (HEP187170; 26 years, female) (lower panel) were assessed for functionality by histochemical and immunohistochemical analyses. Serial liver sections were stained for H&E, PAS, CYP3A4 and MRP2. Bar = 100 μm.

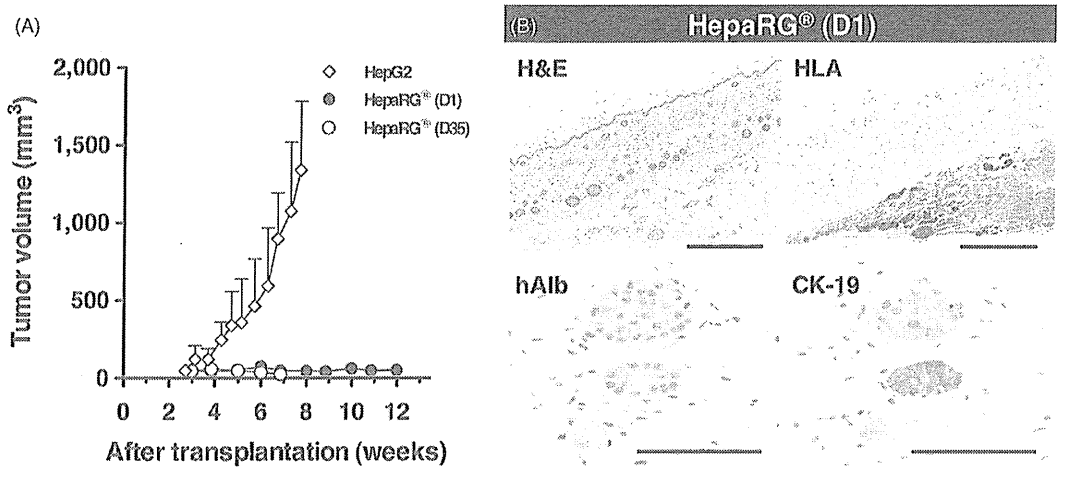

Figure 4. Tumorigenic potency of HepaRG® cells in NOG mice. (A) The growth potential of HepaRG® cells was evaluated in NOG mice. A total of 1×10^6 cells were subcutaneously transplanted into NOG mice. D1 and D35 in HepaRG® stage indicate the number of days after seeding. A total of 1×10^4 HepG2 cells were used as positive control for s.c. transplantation. (B) Histologic and immunohistochemical analyses of D1 HepaRG® xenografts in NOG mouse. Twelve weeks after transplantation, the xenografts were processed for H&E staining, HLA, hAlb and CK-19 staining. Bar = 500 μm. Bar = 50 μm.

they were abundantly expressed, mirroring the degree of cellular differentiation, with the exception of CYP1A1 (Aninat et al., 2006; Antherieu et al., 2010).

Most cytochrome P450 enzymes appear either at or near birth or between 2 and 4 weeks following birth; in contrast, CYP1A1 is expressed very early in development in rodents (Rich & Boobis, 1997) and humans (Yang et al., 1995). Because the differentiation stages of HepaRG® cells could be induced after exposure to beta-naphthoflavone (BNF), phenobarbital (PB) and rifampicin (RIF), to express both mRNA and CYP protein activities, they could be used in screens as a substitute for and/or in complement to primary hepatocytes for CYP induction studies (Aninat et al., 2006; Antherieu et al., 2010; Gerets et al., 2012). Because of the responses of the HepaRG® cells in these systems, they were subsequently evaluated *in vivo* to determine whether or not they could serve as an alternative to primary hepatocytes.

We transplanted four distinct differentiation stages of HepaRG® cells into the livers of TK-NOG mice. Although HepaRG® cells in any differentiation stage could engraft and proliferate within the recipient livers, the HepaRG® cells in the proliferative stage (D1) differentiated only to Alb-negative/CK-19-positive biliary-like cells in the recipient mouse livers. These results presented here have also indicated that the differentiation program from progenitors toward hepatocyte lineage will not occur in *in vivo* microenvironments. Because HepaRG® cells drastically change their morphological and molecular biological characteristics *in vitro* after reaching confluency, high-density culture conditions induce and preserve the differentiation status of

RIGHTSLINK

Xenobiotica Downloaded from informahealthcare.com by 218.33.133.54 on 01/24/14
For personal use only.